Sudan University of Science and Technology

College of graduate studies

Utilization of Laser Induced Breakdown Spectroscopy (LIBS) to Detect the Heavy Metals and their Concentrations in Dairy Products Waste Water

إستخدام مطيافية الإنهيار الكهربي المستحث بالليزر لإستكشاف المعادن الثقيلة وتراكيزها الموجودة فى عينات مختلفة من مياه منتجات الألبان

A thesis submitted for the fulfillment of the requirements for the degree of Doctor of Philosophy in Laser Applications in physics

By:

Maria Mohammed Ossman Taha

Supervised by:

Prof. Dr. Nafie A. Almuslet

November 2015

الآيــة

قال الله تعالى:

اقْرَأْ بِاسْمِ رَبِّكَ الَّذِي خَلَقَ(1) خَلَقَ الْإِنسَانَ مِنْ عَلَقٍ(2)

اقْرَأْ وَرَبُّكَ الْأَكْرَمُ(3) الَّذِي عَلَّمَ بِالْقَلَمِ(4) عَلَّمَ الْإِنسَانَ

مَا لَمْ يَعْلَمْ(5).

صدق الله العظيم

العلق (1-5)

Acknowledgement

First, I thank Allah, who gave me the opportunity and strength to carry out this work. My greatest thanks are to my parents who bestowed ability and strength in me to complete this work. I would like to express my gratitude to **Professor. Nafie A. Almuslet,** for guidance and support throughout my thesis work. He has been a constant source of inspiration to me throughout the period of this project. I consider myself extremely fortunate for having the opportunity to learn and work under his supervision over the entire period.

I would also take this opportunity to express my gratitude and sincere thanks to Austaza **Siham M. Osman** for her help and support.

Thanks for the staff of laser institute, Sudan University for their help, inspiration, and moral support.

I am also very thankful to **Eng. Walid Muhammad Elfatih**, Control & Embedded system Engineer, Military Industry Corporation (ZEC), for his valuable suggestions.

I take this opportunity to express my profound sense of gratitude and respect to my colleagues, and all those who helped me through the duration of this project work.

Dedication

I would like to dedicate my dissertation to:

my mother,

my Father,

my brothers and sisters,

for their love, patience, and support.

Table of Contents

List of Table

List of Figure

Abstract

In this work, Laser Induced Breakdown Spectroscopy (LIBS) has been used to investigate, and calculate the concentrations, of heavy metals in waste water collected from dairy products processing plants in Khartoum state during the period from 2013 to 2015.

Five industrial waste water samples, collected from diary product plants, were used as study samples.

The breakdown of the samples was induced by focusing a pulsed Nd: YAG laser at 532 nm, 2Hz Rpetion Rate, pulse duration of 10 ns, with pulse energies: 30, 60, 80, and 100 mJ, respectively. The emission spectra of the samples plasma were collected via optical fiber and analyzed by Ocean Optics LIBS 4000- spectrometer. The recorded spectra of the samples were analyzed using NIST data.

The analysis of the spectra showed considerable amounts of neutral atoms like Na, Co, Cu, Fe, Cs, Hg, Pr, Cr, Fe, Ti elements in addition to the ions: (Co^{+1} , Cu^{+1}, Cs^{+1} ,Fe^{+1} , Ba^{+2} , Cr^{+1} , Mg^{+2}, and Mn^{+1} ions.

The concentrations of some heavy metals (Fe, Hg, Cr, Ti, Mn, Mg) were calculated using the calibration curves based on the emission spectra of known concentrations of the some elements.

At 30 mJ, (Fe, Hg, Cr, Ti, Mn) were appeared with different concentrations, while Cr, Hg, and Ti were appeared with high concentrations in the five samples, where Ti had the highest concentration. At 60 mJ, the element of (Fe, Cr, Ti, Mg) were appeared with low concentrations relative to the concentrations of the same metals at 30 mJ,

It can be concluded that LIBS technique proved to be, fast accurate technique in the detection of heavy metals and determine its concentrations in liquid samples.

A portable LIBS system for online analysis of contaminated sites with heavy metals can be recommended for improvement of the environment and controlling the pollution at industrial areas. Also the study recommended the establishment of a correlation between the laser power density and the ionization energy for each element.

المستخلص

في هذه الدراسة تم إستخدام تقانة الإنهيار الكهربي بواسطة الليزر(LIBS) للكشف عن العناصر الثقيله وحساب تراكيزها في عينات مختلفه من مخلفات مياه بعض مصانع منتجات الألبان في ولاية الخرطوم خلال الفترة من 2013 الى 2015.

تم تشعيع هذه العينات بواسطة ليزر النيوديميوم – ياق النبضي ذي الطول الموجي 532 نانو متر بطاقات نبضه 30, 80,60 , 100ملي جول وبزمن نبضه قدره 10 نانو ثانيه وتردد 2 هيرتز وتكرار التشعيع 20 مرة لكل عينة .

تم تسجيل أطياف الأنبعاث للعينات بواسطة جهاز المطياف نوع (LIBS 4000 - Spectrometer), وباستخدام قاعدة بيانات التحليل الطيفي للعناصر (Atomic Spectra Database line) تم الكشف عن الكوبالت, النحاس, الحديد, الزئبق, البرامسيوم, الكروم, التيتانيوم, الصوديوم, السيزيوم, المنجنيز والماغنسيوم وايوناتها الموجودة في طيف الإنبعاث لكل عينة.

تم حساب تراكيز بعض هذه العناصر للعينات المشعة بـ 30, 60 ملي جول وهي : الحديد, الزئبق, الكروم , التيتانيوم, المنجنيز والماغنسيوم وتم تحديدها حسب نسبها في الخمس عينات. وجد أن عناصر الكروم ,الزئبق والتيتانيوم تتواجد بتراكيز عالية في كل العينات وكان التيتانيوم اكثرها تركيزاً في العينة الثالثة وأيضا عندما شععت العينات ب 60 ملي جول وجد أن الحديد, الكروم, الزئبق والماغنسيوم متواجده بتراكيز أقل مقارنة معها عندما شععت ب 30 ملي جول.

من النتائج المتحصله يستنتج أن طريقة الأنبعاث المستحث بالليزر (LIBS) تعتبر طريقة كفؤة و سريعة ودقيقة للكشف عن العناصر الثقيلة وحساب تراكيزها في العينات السائلة.

في نهاية البحث تمت التوصية بتصميم نظام متكامل محمول ميدانيا لإستخدام تقانة الانبعاث المستحث بالليزر (LIBS) للكشف عن العناصر الثقيلة في عينات مختلفة من البيئة. كما تم إقتراح عمل علاقة مابين كثافة القدره لليزر المستخدم وطاقة التأين لكل عنصر من العناصر الثقيلة.

Chapter one

Laser spectroscopy, an overview

Chapter one

Laser spectroscopy, an overview

1.1 Introduction:

Most of our knowledge about the structure of atoms and molecules is based on spectroscopic investigations. Thus spectroscopy has made an outstanding contribution to the present state of atomic and molecular physics, to chemistry, and to molecular biology. Information on molecular structure and on the interaction of molecules with their surroundings may be derived in various ways from the absorption or emission spectra generated when electromagnetic radiation interacts with matter.

Wavelength measurements of spectral lines allow the determination of energy levels of the atomic or molecular system. The line intensity is proportional to the transition probability, which measures how strongly the two levels of a molecular transition are coupled. Since the transition probability depends on the wave functions of both levels, intensity measurements are useful to verify the spatial charge distribution of excited electrons, which can only be roughly calculated from approximate solutions of the Schrödinger equation (Wolfgang Demtröder, 2008).

From 1960 onwards, the increasing availability of intense, monochromatic laser sources provided a tremendous impetus to a wide range of spectroscopic investigations. Laser radiation is very much more intense, and the linewidth much smaller, than that from, for example, a mercury arc, which was commonly used as a Raman source before 1960 (Michael Hollas, 2004).

In recent years, laser based technologies became important or even dominant in industrial applications such as welding or cutting. Further possibilities of processing, innovation, and advancement of laser material treatments are still in

progress and very challenging. Laser-based analysis, spectroscopy, or metrology are well known and established methods (Wolfgang, 2008).

It may be apparent that, when lasers are used as spectroscopic sources, one can no longer think in terms of generally applicable experimental methods. A wide variety of ingenious techniques have been devised using laser sources, (Jerry, 1997).

Laser spectroscopy has a great contribution to the discovery of the hundreds of lasers nowadays, and this allowed the field to be expanding very rapidly and involve a very large number of fields, (Franz Mayinger, 1994).

1.2 The study objectives:

The objectives of this research work are to detect the heavy metals in industrial water samples, collected from different dairy product plants and to determine their concentrations using laser induced breakdown spectroscopy (LIBS) technique. The Study was conducted with an aim to keep the experimental setup as simple as technically possible and to improve the capabilities of this technique for applications to various samples of environmental significance.

1.3 The thesis structure:

Chapter one deals with an overview of laser spectroscopy and the objectives of this research work. In chapter two, descriptions of Laser Induced Breakdown Spectroscopy, principles, capabilities, instrumentation and literature review are presented. Experimental setup, components of LIBS setup, sample collection and preparation procedure are presented in chapter three. In chapter four, results and discussion beside the conclusions and recommendations were review.

1.4 Absorption, Induced, and Spontaneous Emission

Assume that molecules with the energy levels $\boldsymbol{E_1}$ and E_2 have been brought into the thermal radiation field. If a molecule absorbs a photon of energy $h\nu = E_2 - E_1$, it is excited from the lower energy level E_1 into the higher level E_2 (Fig. 1.1). This

process is called induced absorption. The probability per second that a molecule will absorb a photon, dP_{12}/dt, is proportional to the number of photons of energy $h\nu$ per unit volume and can be expressed in terms of the spectral energy density $\rho(\nu)$ of the radiation field as:

$$\frac{d}{dt} P_{12} = B_{12}\,\rho(\nu) \qquad (1.1)$$

The constant factor B_{12} is the Einstein coefficient of induced absorption. It depends on the electronic structure of the atom, i.e. on its electronic wave functions in the two levels 1 and 2. Each absorbed photon of energy hν decreases the number of photons in one mode of the radiation field by one. The radiation field can also induce molecules in the excited state E_2 to make a transition to the lower state E_1 with simultaneous emission of a photon of energy hν. This process is called induced (or stimulated) emission. The induced photon of energy hν is emitted into the same mode that caused the emission. This means that the number of photons in this mode is increased by one. The probability dP_{21}/dt that one molecule emits one induced photon per second is in analogy to (1.2)

$$\frac{d}{dt} P_{12} = B_{21}\,\rho(\nu) \qquad (1.2)$$

The constant factor B_{21} is the Einstein coefficient of induced emission.

An excited molecule in the state E_2 may also spontaneously convert its excitation energy into an emitted photon hν. This spontaneous radiation can be emitted in the arbitrary direction k and increases the number of photons in the mode with frequency ν and wave vector k by one. In the case of isotropic emission, the probability of gaining a spontaneous photon is equal for all modes with the same frequency ν but different directions k. The probability per second dP^{Spon}_{21}/dt that a photon $h\nu = E_2 - E_1$ is spontaneously emitted by a molecule, depends on the

structure of the molecule and the selected transition 2 to 1, but it is independent of the external radiation field (Wolfgang Demtröder, 2008).

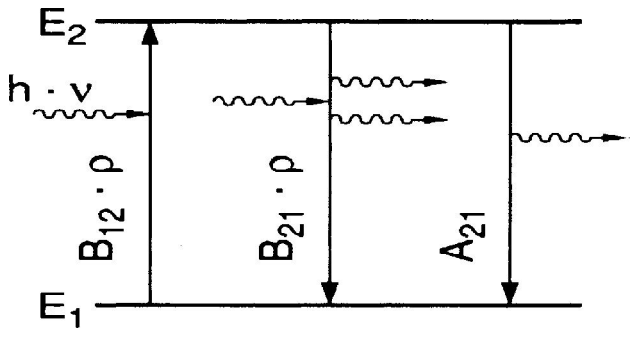

Fig (1.1): Schematic diagram of the interaction of a two-level system with a radiation field

1.5. Basic Elements of a Laser:

A laser is a device that generates light by a process called stimulated emission. The acronym LASER stands for Light Amplification by Stimulated Emission of Radiation. A laser consists of essentially three components (Fig. 1.2):

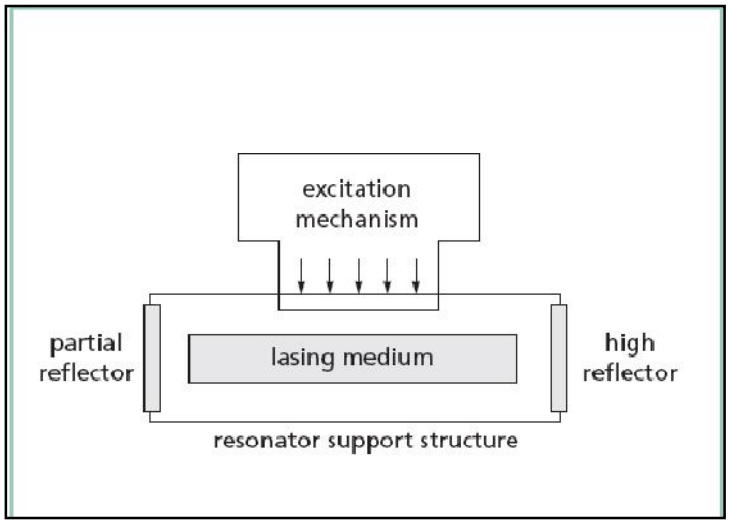

Fig (1.2): Schematic diagram of a basic laser:

• The active medium, which amplifies an incident electromagnetic (EM) wave;

• The excitation mechanism, which selectively pumps energy into the active medium to populate selected levels and to achieve population inversion;

• The optical resonator that consist of example, of two opposite mirrors,which stores part of the induced emission that is concentrated within a few resonator modes(Wolfgang Demtröder, 2008).

1.5.1. The active medium:

Active medium (gain medium, laser medium). The active medium is able to amplify electromagnetic radiation. The activemedium, located inside a resonator, fills out a resonator partly or completely, (Karl F. Renk, 2011).

An atom (or a molecule) used in a laser has two laser levels, beside other energy levels. We ignore for the moment the other levels and describe an atom as a two levels atomic system and accordingly an ensemble of atoms as an ensemble of two-level atomic systems. We introduce the following notation.

• Level 2 (energy E_2) = upper laser level.

• Level 1 (energy E_1) = lower laser level.

• $E_{21} = E_2 - E_1$, energy difference between the two laser levels Dtransition energy.

• N_2 population of level 2= density of excited two-level atomic systems = number density (number per unit of volume) of excited two-level atomic systems.

• N_1 = population of level 1= density of unexcited two-level atomic systems.

• $N_2 - N_1$ = population difference.

• $N_1 + N_2$ = density of two-level atomic systems.

Monochromatic electromagnetic radiation of frequency _ can interact with a two level atomic system if Bohr's energy-frequency relation

$$h\upsilon = E_{21} = E_2 - E_1$$

holds, that is, if the photon energy $h\upsilon$ of the photons of the radiation field is equal

to the energy difference E_{21}. But because of lifetime broadening of the upper level, a two-level atomic system can also interact if hυ is unequal to E_{21}.

Two processes are competing with each other in a laser, absorption and stimulated emission of radiation (Karl F. Renk, 2011).

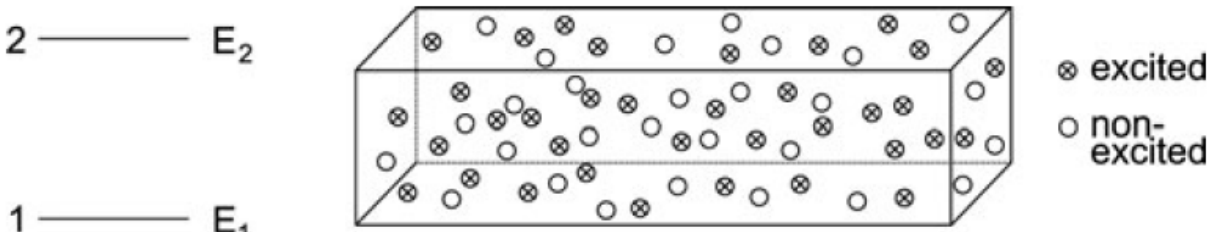

Fig. (1.3): Two-level atomic system and ensemble of two-level atomic systems

1.5.2. The excitation mechanism:

The energy pump (e.g., flash lamps, gas discharges, or even other lasers) generates a population distribution *N(E)* in the laser medium, which strongly deviates from the Boltzmann distribution that exists for thermal equilibrium. At sufficiently large pump powers the population density $N(E_k)$ of the specific level E_k may exceed that of the lower level (E_i).

For such a population inversion, the induced emission rate $N_k B_{ki}\, \rho(\nu)$ for the transition $E_k \rightarrow E_i$ exeeds the absorption rate $N_i\, B_{ik}\, \rho(\nu)$ (Wolfgang Demtröder, 2008).

1.5.3. Population Inversion:

Atomic energy states are much more complex than indicated by the description above. There are many more energy levels, and each one has its own time constants for decay. The four-level energy diagram shown in figure below is representative of some real lasers. The electron is pumped (excited) into an upper level E_4 by some mechanism (for example, a collision with another atom or

absorption of high-energy radiation). It then decays to E_3, then to E_2, and finally to the ground state E_1. Let us assume that the time it takes to decay from E_2 to E1 is much longer than the time it takes to decay from E_2 to E_1. In a large population of such atoms, at equilibrium and with a continuous pumping process, a population inversion will occur between the E_3 and E_2 energy states, and a photon entering the population will be amplified coherently, (www.mellesgriot.com).

1.5.4 The Resonator:

Although with a population inversion we have the ability to amplify a signal via stimulated emission, the overall single-pass gain is quite small, and most of the excited atoms in the population emit spontaneously and do not contribute to the overall output. To turn this system into a laser, we need a positive feedback mechanism that will cause the majority of the atoms in the population to contribute to the coherent output. This is the resonator, a system of mirrors that reflects undesirable (off-axis) photons out of the system and reflects the desirable (on-axis) photons back into the excited population where they can continue to be amplified If laser system shown in figure (1.4) the lasing medium is pumped continuously to create a population inversion at the lasing wavelength. As the excited atoms start to decay, they emit photons spontaneously in all directions. Some of the photons travel along the axis of the lasing medium, but most of the photons are directed out the sides. The photons traveling along the axis have an opportunity to stimulate atoms they encounter to emit photons, but the ones radiating out the sides do not. Furthermore, the photons traveling parallel to the axis will be reflected back into the lasing medium and given the opportunity to stimulate more excited atoms. As the on-axis photons are reflected back and forth interacting with more and more atoms, spontaneous emission decreases, stimulated emission along the axis predominates, and we have a laser (www.mellesgriot.com).

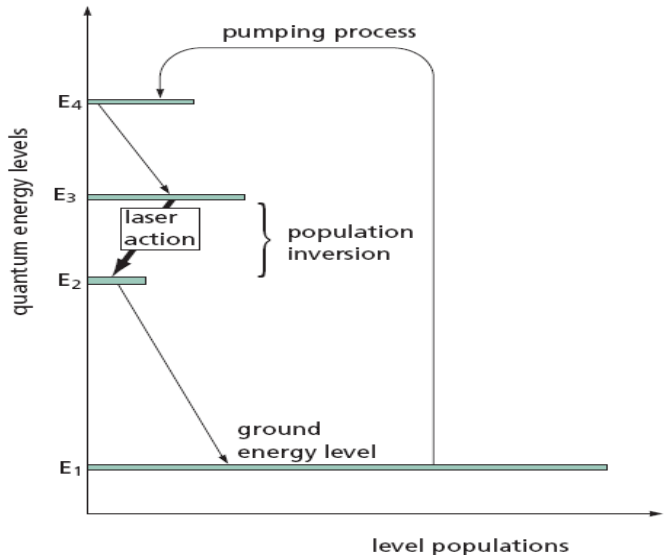

Fig (1.4): four-level laser pumping system

1.6. Generation of Ultra short Laser Pulses:

Lasers are divided into continuous wave lasers (CW) and pulsed lasers. In CW lasers, the intensity of the emitted light is constant as a function of time. In the CW regime, the gain is equal to losses after the round-trip time in the resonator. When the gain achieved after the round-trip time in the resonator, every subsequent passage leads to further amplification of the light emitted by the laser. This condition is required for pulsed lasers, (Halina Abramczyk , 2005).

The temporal pulse duration in cw lasers goes to infinity. In pulsed lasers, the energy is released in the form of a short pulse of light. Initially, in 1960, laser pulses were around 10 ms long with a peak power of kilowatts. Shortly after 1960, the Q-switching technique reduced the pulse duration by a factor of 10^4 to nanoseconds, with peak powers of megawatts.

In 1964, the development of the mode locking technique reduced the pulse duration to picoseconds and pushed the peak power up to giga watts. Shortly thereafter, pulses of just a few femtoseconds were produced using colliding-pulse

modelocking. Until about a decade ago, dye lasers were used exclusively to generate ultrashort pulses. Now, they have been replaced by the more convenient technology of solid-state lasers and fiber lasers. The lasers working in the modelocking regime represent a special group of continuous wave lasers, (Halina Abramczyk , 2005).

1.7. Basics of Spectroscopy:

Any matter in our universe is composed of atoms or molecules (or may be ions) or a collection of them. Each atom, molecule or ion has its unique states of energy (finger print). These energy states (levels) are, usually, represented by horizontal lines, each one represents certain probable state of energy of that matter. Actually these energy levels are the (identity) of the matter because one cannot find two matters with similar energy states. If, for any reason, the atom or the molecule exchanges energy with an external source of energy then its energy state will be changed. In this case the system suffered from (transition) in its energy states and the process is represented by vertical arrow. When the system gained external energy, the arrow is directed up and the process is named (absorption). While if the system loss energy the arrow is directed down and the process is known as (emission). Spectroscopy was originally the study of interaction between radiation and matter as a function of wavelength (λ). Historically it was referred to visible light dispersed according to its wavelength e.g. by a prism, later it expands to comprise any measurement of a quantity as a function of wavelength, frequency (υ) or energy (E) as a variable, (Leon J. Radziemski, Richard W. Solarz, and Jeffrey A.Paisner, 1987).

$$E = h\upsilon = hc / \lambda \qquad (1.3)$$

Where: h : Plank's constant (6.626×10^{-34} J·s, υ : light wave frequency

c :speed of light (3×10^{8} m/s) and λ : light wavelength

There are two types of spectroscopy:

(i) Atomic spectroscopy:

The study of transitions, in absorption or emission, between electronic states of an atom, is atomic spectroscopy. It deals with the interaction of electromagnetic radiation with atoms which are most commonly in their lowest energy state, (Leon J. Radziemski, Richard W. Solarz, and Jeffrey A.Paisner, 1987).

Atomic spectra involve only transitions of electrons from one electronic energy level to another. There are two types of atomic spectroscopy:

- Atomic absorption spectroscopy (AAS).
- Atomic emission spectroscopy (AES).

(ii) Molecular Spectroscopy:

This deals with the interaction of electromagnetic radiation with molecules. The results are transitions between rotational and vibrational energy levels in addition to electronic transitions. Absorption of a photon may excite the molecule to a higher electronic vibrational and / or rotational energy level. There are many transitions that might give rise to absorption (Leon J. Radziemski, Richard W. Solarz, and Jeffrey A.Paisner, 1987).

1.7.1: Atomic absorption spectroscopy:

The first assumption in spectroscopic measurements is that Beer's law relationship applies between a change in spectrometer response and the concentration of analyte material present in a sample specimen. The Bouguer, Lambert, and Beer relationship assumes that the transmission of a sample within an incident beam is equivalent to 10 exponent the negative product of the molar extinction coefficient (in L. mol^{-1} cm^{-1}), multiplied by the concentration of a molecule in solution (in mol. L^{-1}) times the path length (in cm) of the sample in solution (Leon J. Radziemski, Richard W. Solarz, and Jeffrey A.Paisner, 1987). There are some obvious (and not so obvious) problems with this assumption. The main difficulty in

the assumed relationship is that the molecules often interact, and the extinction coefficient (absorptivity) 1.4)

$$T = I/I_0 = I_0 e^{-c\varepsilon l} \quad (1.4)$$

where T is the transmittance, I_o is the intensity of incident energy, I is the intensity of transmitted light, ε is the molar extinction coefficient (in L. mol^{-1} cm^{-1}), c is the concentration (in mol. L^{-1}) and ⌊ is the path length (in cm), (Jerry Workman, 1997).

1.7.2 Atomic Emission Spectroscopy (AES):

Atomic Emission Spectroscopy, AES, is the measurement of light emissions from excited atoms. The concentration of an analyte element can be determined from the quantitative measurement of these emissions. A source such as a plasma, flame, or discharge is used to provide the energy to atomize and excite analyte atoms and promote them to higher energy levels. The optical emission corresponds to the excited atoms returning to lower energy level (s) and emitting light that is detected by a photon detector system.

In AES, the process begins with sample introduction. Sample introduction techniques vary with AES but the usual procedure for liquid samples is to aspirate the sample solution and convert it into an aerosol to introduce small droplets of the analyte into the atomizer. This sample introduction method helps prevent the atomizer from being extinguished or from incompletely removing solvent. The heat of the atomizer desolvates or removes excess solvent/water from the sample droplets through volatilization and evaporation processes and dries the sample particles.1 In atomization, chemical bonds are broken and free atoms are produced. These free atoms become excited and gain energy from collisions in the atomizer. The atoms leave the ground state and are promoted to an excited state where they emit light upon returning to lower energy levels, (David A. Cremers, Leon J.

Radziemski, 2006). The excited atoms return to lower energy states and eventually to the ground state due to the loss of energy. The relationship that exists between atoms in an excited state and atoms in a lower state is based on the Boltzmann equilibrium. The Boltzmann equilibrium is described in the following expression:

Boltzmann Equation:

$$N_1/N_0 = e^{-\Delta E/KT} \quad (1.5)$$

N_1 = number of atoms in the upper state

N_0 = number of atoms in the lower state

E = energy difference between upper and lower states, cm^{-1}

k = Boltzmann constant, J/K

T = absolute temperature, K

For degeneracy as in figure 2, the equation is:

$$N_1/N_0 = (g_1/g_0)e^{-\Delta E/KT} \quad (1.6)$$

1. 8 The use of lasers in spectroscopy:

1. 8.1 Laser AES:

As soon as the laser was developed in the early 1960s, spectrochemists began investigating its potential uses. An early observation was that a pulsed laser could produce a small plasma in air. The emission from that plasma From 1960 onwards, increasing availability of intense, monochromatic laser sources provided a tremendous impetus to a wide range of spectroscopic investigations, (J. Michael Hollas, 2004).

From 1960 to 1980 the analytical capability was so inferior to that of the conventional spark and laser technology was in its infancy, so that the technique was less favored than a related one – laser ablation into a conventional plasma

source. Here the laser was used to vaporize a small amount of sample for analysis by, for example, the conventional electrode spark. However, that was not the only way the laser could be used in spectrochemistry.

The development of tunable dye lasers meant that one could illuminate a prepared source of atoms with radiation resonant with a transition in one of the atomic species. Then either the absorption of the laser beam or the laser-induced fluorescence could be used as an analytical signal. These techniques discriminated against background and increased the signal to noise considerably by recycling the same atoms many times. Sometimes the atoms were placed in the laser cavity itself. The intra-cavity absorption technique was a very sensitive spectrochemical method, if difficult to employ generally (David A. Cremers, Leon J. Radziemski, 2006).

Both absorption and fluorescence are used in many applications. However, because the laser needs to be tuned to a specific transition in a specific species, it is not as broadly useful as a hot plasma in which a variety of species can be excited and monitored simultaneously, (David A. Cremers, Leon J. Radziemski, 2006).

A useful way of changing the wavelength of some lasers, for example the CO_2 infrared laser, is to use isotopically substituted material in which the wavelengths of laser transitions are appreciably altered, (J. Michael Hollas, 2004).

In regions of the spectrum where a tunable laser is available it may be possible to use it to obtain an absorption spectrum in the same way as a tunable klystron or backward wave oscillator is used in microwave or millimetre wave spectroscopy. Absorbance is measured as a function of frequency or wavenumber. This technique can be used with a diode laser to produce an infrared absorption spectrum. When electronic transitions are being studied, greater sensitivity is usually achieved by monitoring secondary processes which follow, and are directly related to, the absorption which has occurred. Such processes include fluorescence, dissociation,

or pre-dissociation, and, following the absorption of one or more additional photons, ionization. The spectrum resulting from monitoring these processes usually resembles the absorption spectrum very closely.

It is apparent that, when lasers are used as spectroscopic sources, we can no longer think in terms of generally applicable experimental methods, (J. Michael Hollas, 2004).

1.8.2 Laser Raman Spectroscopy:

Raman spectroscopy is a spectroscopic technique based on inelastic scattering of monochromatic light, usually from a laser source. Inelastic scattering means that the frequency of photons in monochromatic light changes upon interaction with a sample. Photons of the laser light are absorbed by the sample and then reemitted. Frequency of the reemitted photons is shifted up or down in comparison with original monochromatic frequency, which is called the Raman effect.

This shift provides information about vibrational, rotational and other low frequency transitions in molecules. Raman spectroscopy can be used to study solid, liquid and gaseous samples.

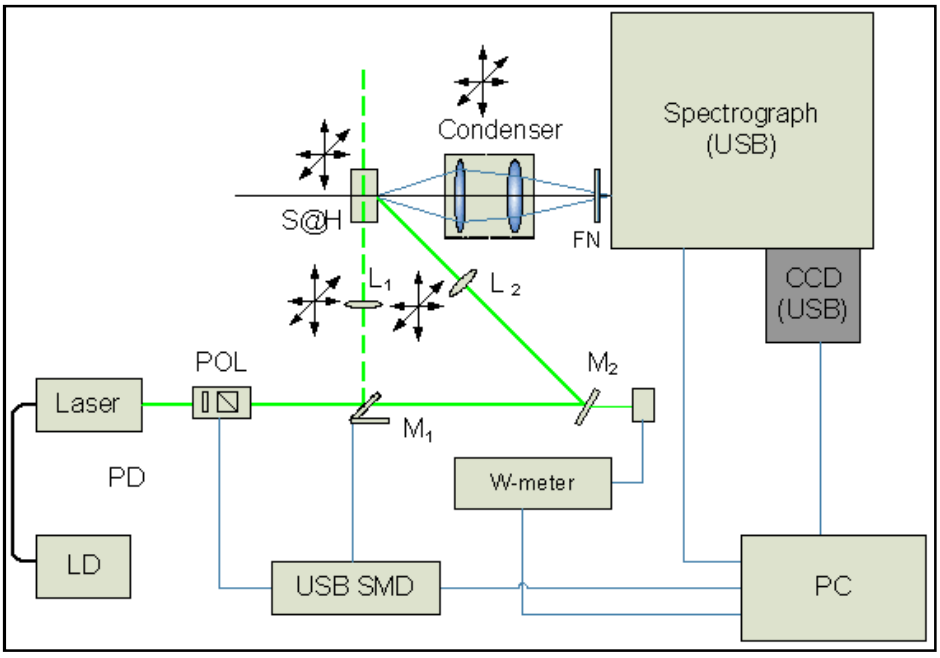

Fig (1.5): laser Raman system

The Raman effect is based on molecular deformations in electric field E determined by molecular polarizability α. The laser beam can be considered as an oscillating electromagnetic wave with electrical vector E. Upon interaction with the sample it induces electric dipole moment P = α E which deforms molecules. Because of periodical deformation, molecules start vibrating with characteristic frequency υ_m.

For many years Raman spectroscopy has been a powerful tool for the investigation of molecular vibrations and rotations. The introduction of lasers, therefore, has indeed revolutionized this classical field of spectroscopy. Lasers have not only greatly enhanced the sensitivity of spontaneous Raman spectroscopy but they have furthermore initiated new spectroscopic techniques, based on the stimulated Raman effect, such as coherent anti-Stokes Raman scattering (CARS) or hyper-Raman spectroscopy (J. Demtröder, 2008).

The research activities in laser Raman spectroscopy have recently shown an impressive expansion and a vast literature on this field is available (J. Demtröder, 2008).

The most immediately obvious application of early, essentially non-tunable, lasers was to all types of Raman spectroscopy in the gas, liquid or solid phase (J. Michael Hollas, 2004).

As a result, weaker Raman scattering can now be observed and higher resolution is obtainable. In addition to carrying out conventional Raman experiments with laser sources new kinds of Raman experiments became possible using Q-switched, giant pulse lasers to investigate effects which arise from the non-linear relationship between the induced electric dipole and the oscillating electric field. These are grouped under the general heading of non-linear Raman effects. For branches of spectroscopy other than Raman spectroscopy most laser sources may appear to have a great disadvantage, that of non-tunability (J. Michael Hollas, 2004).

Amplitude of vibration is called a nuclear displacement. In other words, monochromatic laser light with frequency υ_0 excites molecules and transforms them into oscillating dipoles. Such oscillating dipoles emit light of three different frequencies (Fig.1.5) when:

1. A molecule with no Raman-active modes absorbs a photon with the frequency $\upsilon 0$. The excited molecule returns back to the same basic vibrational state and emits light with the same frequency υ_0 as an excitation source. This type if interaction is called an elastic Rayleigh scattering.

2. A photon with frequency υ_0 is absorbed by Raman-active molecule which at the time of interaction is in the basic vibrational state. Part of the photon's energy is transferred to the Raman-active mode with frequency υ_m and the resulting frequency of scattered light is reduced to $\upsilon_0 - \upsilon_m$. This Raman frequency is called Stokes frequency, or just "Stokes".

3. A photon with frequency υ_0 is absorbed by a Raman-active molecule, which, at the time of interaction, is already in the excited vibrational state. Excessive energy of excited Raman active mode is released, molecule returns to the basic vibrational state and the resulting frequency of scattered light goes up to $\upsilon_0 + \upsilon m$. This Raman frequency is called Anti-Stokes frequency, or just "Anti-Stokes".

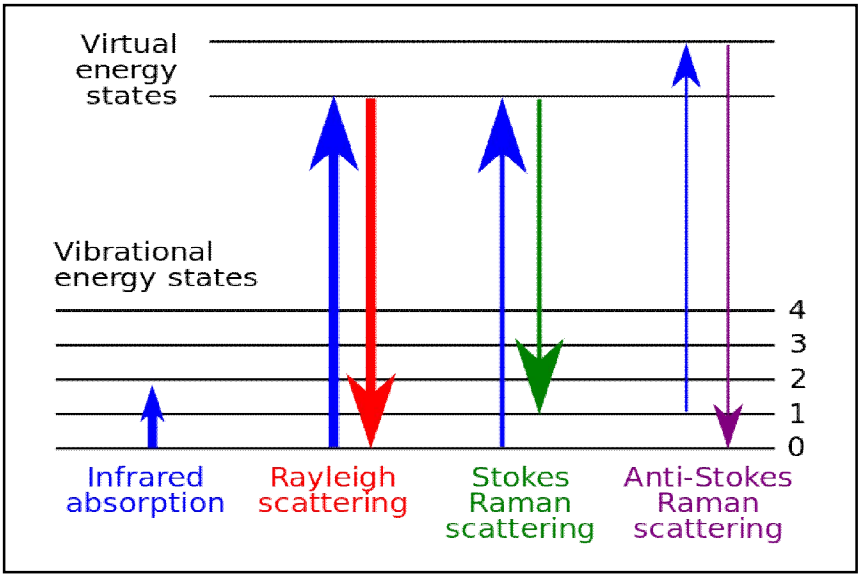

Figure (1.6): Stimulated Raman transitional schemes

About 99.999% of all incident photons in spontaneous Raman undergo elastic Rayleigh scattering. This type of signal is useless for practical purposes of molecular characterization. Only about 0.001% of the incident light produces inelastic Raman signal with frequencies $\upsilon_0 \pm \upsilon_m$. Spontaneous Raman scattering is very weak and special measures should be taken to distinguish it from the predominant Rayleigh scattering. Instruments such as notch filters, tunable filters, laser stop apertures, double and triple spectrometric systems are used to reduce Rayleigh scattering and obtain high-quality Raman spectra. (www.piactton.com,2015)

1.8.3. Laser induced fluorescence (LIF):

Is an emitted from electronically excited levels that are populated by absorption of photons, typically in the ultraviolet and visible spectral region. (Christof Schulz, Volker Sick, 2004).

In Laser induced fluorescence (LIF) technique the laser beam is formed into a thin light sheet by a set of lenses, and this light sheet entering the observation volume. The fluorescence is captured by a collecting lens and imaged on to the detector surface; the data of the images is transferred from the camera to the control unit installed in a computer (Hollars M.J., 2004).

The emitted radiation is characteristic for the concentration and temperature of the regarded species. Fig (1.6) show the experiment use in this technique.

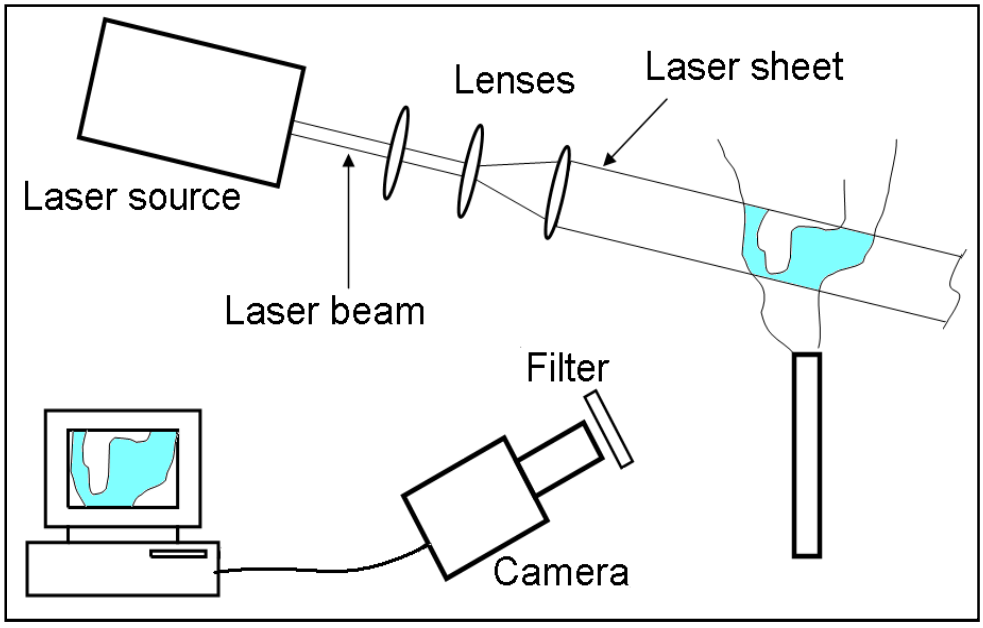

Fig (1.7): The experimental setup of LIF

1.8.4. Mass spectroscopy:

The basic principle of mass spectrometry (MS) is to generate ions from either inorganic or organic compounds by any suitable method, to separate these ions by their *mass-to-charge ratio* (*m/z*) and to detect them qualitatively and quantitatively by their respective *m/z* and abundance. The analyte may be ionized thermally, by electric fields or by impacting energetic electrons, ions or photons. The ... ions can be single ionized atoms, clusters, molecules or their fragments or associates. Ion separation is effected by static or dynamic electric or magnetic fields." Although this definition of mass spectrometry dates back to 1968 when organic mass spectrometry was in its infancy, it is still valid. However, two additions should be made. First, besides electrons, (atomic) ions or photons, energetic neutral atoms and heavy cluster ions can also be used to effect ionization of the analyte. Second, as demonstrated with great success by the time-of-flight analyzer, ion separation by *m/z* can be effected in field free regions, too, provided the ions possess a well defined kinetic energy at the entrance of the flight path. (L. J. Radziemski, Spectrochim. Acta, 2002).

A mass spectrum is the two-dimensional representation of signal intensity (ordinate) versus m/z (abscissa). The intensity of a peak, as signals are usually called, directly reflects the abundance of ionic species of that respective m/z ratio which have been created from the analyte within the ion source.

The mass-to-charge ratio, m/z, is dimensionless by definition, because it calculates from the dimensionless mass number, m, of a given ion, and the number of its elementary charges, z. The number of elementary charges is often, but by far not necessarily, equal to one. As long as only singly charged ions are observed (z = 1) the m/z scale directly reflects the m scale. However, there can be conditions where doubly, triply or even highly charged ions are being created from the analyte depending on the ionization method employed. The location of a peak on the

abscissa is reported as at m/z. The distance between peaks on that axis has the meaning of a neutral loss from the ion at higher m/z to produce the fragment ion at lower m/z. Therefore, theamount of this neutral loss is given as “x u”, where the symbol u stands for unified atomic mass. It is important to notice that the mass of the neutral is only reflected by the difference between the corresponding m/z ratios. This is because the mass spectrometer detects only charged species, i.e., the charge-retaining group of a fragmenting ion. Since 1961 the unified atomic mass [u] is defined as 1/12 of the mass of one atom of nuclide 12C which has been assigned to 12 u exactly by convention.

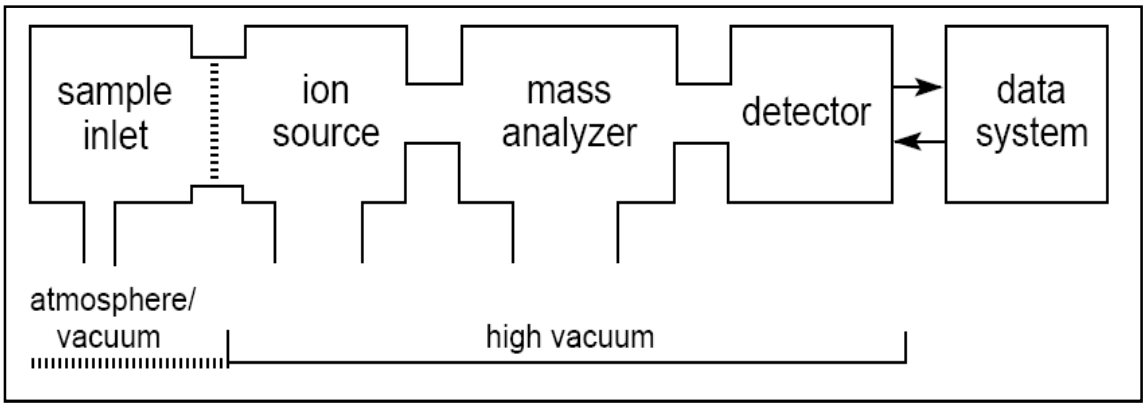

Fig. (1.8) General scheme of a mass spectrometer

1.8.5 Laser induced breakdown spectroscopy (LIBS):

Laser-induced breakdown spectroscopy (LIBS) is an atomic emission spectroscopy. Atoms are excited from the lower energy level to high energy level when they are in the high energy status. The conventional excitation energy source can be a hot flame, light or high temperature plasma. The excited energy that holds the atom at the higher energy level will be released and the atom returns to its ground state eventually. The released energy is well defined for the specific excited atom, and this characteristic process utilizes emission spectroscopy for the

analytical method. LIBS employs the laser pulse to atomize the sample and leads to atomic emission. Compared to the conventional flame emission spectroscopy, LIBS atomizes only the small portion of the sample by the focused laser pulse, which makes a tiny spark on the sample. Because of the short-life of the spark emission, capturing the instant light is a major skill to collect sufficient intensity of the emitting species. Three major parts of the LIBS system are a pulse laser, sample, and spectrometer. Control system is usually needed to manage timing and the spectrum capturing (Fang.Yu Yueh" Jagdish P. Singh, and Hansheng Zhang, 2010). The LIBS has been used for the materials detection and analysis in various applications.

In the next chapter comprehensive review on the LIBS will be shown.

Chapter two

Laser induced breakdown spectroscopy, principles and applications

Chapter two

Laser induced breakdown spectroscopy, principles and applications

2.1 Introduction:

Analytical applications of Laser Induced Breakdown Spectroscopy (LIBS), have been constantly growing thanks to its intrinsic conceptual simplicity and versatility

LIBS is a simple technique that requires optical access to the sample surface and can therefore be used as a fast method for the detection and quantification of the contaminants in various categories of samples. It is an emerging technique for elemental determination in a wide range of environmental samples, metallurgical, metallic and non –metallic solid, sewage sludge, liquid, aerosol, gases and biological samples. (Rosalba Gaudiuso 1, Marcella Dell'Aglio 2, Olga De Pascale, et al., 2010).

Several elements can be measured with this technique simultaneously even at parts per million concentration level.

In this technique, laser pulses are applied for ablation of the samples, resulting in the vaporization and ionization of sample in hot plasma which is finally analyzed by the spectrometer. The elements are identified by their unique spectral signatures. Qualitative and quantitative analysis can be performed by LIBS both by drawing calibration lines and by using calibration-free methods and some of its features, so as fast multi-elemental response, micro-destructiveness, instrumentation portability, have rendered it particularly suitable for analytical applications in the field of environmental science, space exploration and cultural heritage (Hollas M.J., 2004).

Till date, most of the work on quantitative and qualitative analysis using LIBS technique has been focused to solid samples and much less work has been carried out on liquid samples. The main reason for less work on applications of this

technique for analysis of liquid samples is that it is not easy to generate plasma (Wolfang Demtröder, 2008). It could embrace many problems with laser-plasma generation mechanism in liquids, as compared with laser produced plasmas from solid samples. This is due to the low density of liquids as compared to solids and also shock waves associated with vaporization of liquid samples to create aerosol above the liquid surface. These aerosols may disturb the incident laser radiations and plasma emitted light returning to the spectrometer. In addition, these aerosols can damage the optical components employed for guiding the laser beam onto liquid surface for the collection of laser produced plasma emission. It is also probable that laser pulse could induce bubbles inside liquids that are not transparent to laser induced plasma and could affect the reproducibility of the results (Wolfang Demtröder, 2008).

2. 2 LIBS principles:

Since the second part of 20th century, there has been growing concern over the diverse effects of heavy metals on humans and aquatic ecosystems. Environmental impact of heavy metals was earlier mostly attributed to industrial sources. In recent years, metal production emissions have decreased in many countries due to strict legislation, improved cleaning/ purification technology and altered industrial activities. Today and in the future, dissipate losses from consumption of various metal containing goods are of most concern. Therefore, regulations for heavy metal containing waste disposal have been tightened (Wolfang Demtröder, 2008).

The physics of laser-induced breakdown has been studied extensively. The minimum optical power density required to form a plasma is called the breakdown threshold; different types of laser, samples, and ambient conditions will have different breakdown threshold **(**Fang.Yu Yueh" Jagdish P. Singh, and Hansheng Zhang, et al., 2010).

Some capabilities of LIBS are highlighted below:

1) Pollution monitoring in air, soil, sewage sludge, ground and wastewater.

2) Determination of ore composition during mining.

3) Chemical analysis of explosive materials.

4) Forensics and biochemical applications.

5) Detection of radioactive contamination and hazardous materials.

6) Rapid identification of metals and alloys during recycling of scrap materials.

7) On-line compositional analysis of the molten metals.

8) On-line compositional analysis of liquid glass for process control (iron, lead etc).

9) Depth-profiling and compositional analysis of surface coatings (galvanized steel, plastic coating and heavy-metals in paint).

10) On-line monitoring of particulates in air, (Prof. Dr. Alexander Piel, (2010)

From the viewpoint of material processing and nuclear fusion (plasma generation) the main properties of lasers are power density and also time of duration (for pulse lasers). Presently the most commonly used lasers for high-power application and research are:

- the neodymium laser (Nd:YAG or neodymium glass); its wavelength is 1.064 μιη and duration can be from continuous operation (cw) to pulses of a length 170 fs (0.17 ps);

- carbon dioxide laser ($C0_2$); wavelength is 10.6 pm, possible cw and pulse operation.

In different fields of applications the following types of lasers are also used.

- Free Electron Lasers (FEL), hydrogen fluoride lasers (HF), photochemical iodine lasers, excimer lasers, e.g. KrF, X-Ray lasers.

The development of high power laser technology during the last decade is quite significant. This is due to very intensive research connected with laser nuclear fusion. Below we present some examples of laser systems of the highest power,

which were developed for use in nuclear fusion experiments (Wolfgang Demtröder, 2008).

- Antares system (CO_2 laser) - pulses duration is 100 ps, power is 100 TW (10^{14} W).
- NOVA lasers (Nd:YAG) - pulses duration is 100 ps, power is 125 TW,
- DELFIN system (Nd:YAG) - pulses duration is 0.1 ns with energy 50 J,
- PHEBUS - pulses of 1 ps, energy of 1 pulse of a row of 1 kJ (power is 10^{15} W),
- ISKRA-5 (photochemical iodine laser) - 35 kJ energy in pulses of a length 0.25 ns,
- hydrogen-fluoride (HF) lasers - 3 kJ energy in pulses of 30 ns duration,
- AURORA (KrF excimer lasers) - 1.3 kJ energy in pulses of 5 ns duration.

Lasers with such extreme powers and duration times allow to reach, after focusing in vacuum, the power intensities up to 1023 W/m2. This is 20 orders of magnitude brighter than the sunlight power density at the earth. This also implies strange different approach to the analysis of thermophysical processes occurring during interaction of such energy fluxes with materials, (Halina Abramczyk , 2005).

2.3 Elemental Analysis by LIBS:

The use of LIBS for elemental analysis relies on some fundamental assumptions that must be verified, especially when semi-quantitative and quantitative analysis of samples is pursued. First of all the conditions of optically thin plasma and LTE are always the underlying premises for laser induced plasma studies by emission spectroscopy, both for fundamental studies and for analytical applications. The emission intensity I_{ul} of a peak of frequency v_{ul} is related to the number density of excited emitters, Nu by:

$$I_{ul} = \frac{1}{4\pi} N_u A_{ul} h\nu_{ul} G \qquad (2\text{-}1)$$

Where A_{ul} is the spontaneous emission coefficient of the given transition, h is the Planck constant and G is an instrumental factor depending on the experimental set-up used. This relation is valid only when the considered u_l transition is optically thin, that is, not suffering from self-absorption, a condition that can severely affect

low-energy and resonance lines, particularly for high-concentration elements. Several methods can be found in the literature to evaluate and correct self-absorption, and a good practice in analytical LIBS is to select accurately the emission lines to be used for analysis (Rosalba Gaudiuso, Marcella Dell'Aglio, Olga De Pascale, et al., 2010).

All spectroscopic lines involving the ground state should be excluded, because they are the most severely affected by self-absorption phenomena, which alter the spectral line profiles and thus hinder the quantitative determination of major elements. For these elements, lines corresponding to transitions with lower energy level below 6,000 cm^{-1} should also be possibly excluded.

2.4 LIBS advantages and disadvantages:

LIBS, like other methods of AES, is able to detect all elements and have the ability to provide simultaneous multi-element detection capability with low absolute detection limits. In addition, because the laser spark uses focused optical radiation to form the plasma, LIBS exhibits numerous appealing features that distinguish it from more conventional AES-based analytical techniques like inductively coupled plasma mass spectroscopy. These are: simple and rapid or real time analysis, the ablation and excitation processes are carried out in a single step; little-to-no sample preparation, which results in increased throughput and reduction of tedious and time-consuming sample digestion and preparation procedures (this, however,

can lead to a loss of accuracy through contamination). LIBS allow in situ analysis requiring only optical access to the sample. It can also be performed over a great distance, a technique referred to as *remote* sensing. Unlike remote analysis, in which some part of the LIBS system is close to the sample is the method of *stand-off* analysis. Here, the laser pulse is focused on to the sample at a distance using a long focal length optical system (J. Michael Hollas, 2004). Virtually any kind of sample can be analyzed: solids, liquids, aerosols, or gases. LIBS has the ability to analyze extremely hard materials which are difficult to digest such as ceramics, glasses and superconductors (Richard Fitzpatrick, 1987). It is a non-destructive method, very small amount of sample (0.1 μg – 0.1 mg) is vaporized. It provides good sensitivity for some elements (e.g. Cl, F) difficult to monitor with conventional AES methods. In addition, LIBS has adaptability to a variety of different measurement scenarios, e.g. underwater analysis, direct and remote analysis, compact probe with the use of miniature solid state lasers, stand-off analysis. We can summarize LIBS advantages and disadvantages in the following table:

Table (2.1): Advantages and disadvantages of LIBS technique

Advantages	Disadvantages
1- Minimal (no) sample preparation.	1- Variation in the mass ablated caused by changes in the bulk matrix.
2- All states of matter can be analyzed, as well as conductive and nonconductive samples.	2- Difficulty in obtaining matrix matching standards.
3- Very small amount of material is vaporized(around 10 of ng)	
4- Micro analysis is possible with	3- Standard emission disadvantages,

spatial resolution of 1 – 10 μm 5- Atomization and ionization are in one step. 6- Capability of simultaneous multi-element analysis.	such as spectral interference and self absorption.

2.5. Plasma production:

In physics, the word plasma designates a fully or partially ionized gas consisting of electrons and ions. The term plasma was introduced to describe the charge-neutral part of a gas discharge. The equilibrium part of the discharge acted as a kind of sub-stratum carrying particles of special kinds, like high-velocity electrons from thermionic filaments, molecules and ions of gas impurities (Alexander Piel, 2010).

The plasma state is a gaseous mixture of positive ions and electrons. Plasmas can be fully ionized, as the plasma in the Sun, or partially ionized, as in fluorescent lamps, which contain a large number of neutral atoms.

Plasmas resulting from ionization of neutral gases generally contain equal numbers of positive and negative charge carriers. In this situation, the oppositely charged fluids are strongly coupled, and tend to electrically neutralize one another on macroscopic length-scales. Such plasmas are termed quasi-neutral ("quasi" because the small deviations from exact neutrality have important dynamical consequences for certain types of plasma mode). Strongly non-neutral plasmas, which may even contain charges of only one sign, occur primarily in laboratory experiments: their equilibrium depends on the existence of intense magnetic fields, about which the charged fluid rotates (Richard Fitzpatrick, 1987).

Plasmas are generally described as being partially ionized gases due to the ions and atoms that are formed from the atomization and ionization of the sample.

2.6 Inductively Coupled Plasma-AES (ICP-AES):

ICP atomic emission spectroscopy utilizes a plasma as the atomization and excitation source. A plasma is an electrically neutral, partially ionized gas made up of ions, electrons, and atoms. Plasmas are characterized by their electron density and temperature. The temperature of a plasma in ICP-AES usually ranges from 4000-8000 K. Plasmas in AES acquire their energy from an electric or magnetic field and this energy must be maintained for the plasma to be used for AES. In ICP-AES, the energy is acquired from electrical currents produced by electromagnetic induction. In ICP-AES, the stable, high temperature plasma is formed by an ICP torch. The ICP is a continuous plasma meaning it does not form and quickly decay. The density and temperature of the plasma decrease from the core of the plasma outward.

The ICP torch is made of three concentric tubes and is partially enclosed by a water-cooled coil that is powered by a radio frequency generator. The field becomes magnetically activated when the power is turned on and an inert gas such as Argon flows through the torch. The flowing gas becomes electrically conductive when a tesla coil ignites the gas and a plasma is formed. In ICP-AES, the sample is introduced (solid, liquid, or gas) directly inside the plasma and atomization and excitation occur as previously discussed in Flame-AES. An advantage of ICP-AES is the sensitivity of the technique due to the high temperature plasma source. This sensitivity results in good emission spectra for most elements.

2.7 Laser produced plasma:

Plasmas produced by lasers have similar properties as the ICP plasma, but the formation involves focusing a laser to a point in or on the sample and atomizing and ionizing a small portion (ng to μg) of the sample. A laser pulse creates the plasma which is not continuous but is short-lived. Once formed, it quickly decays by expanding out ward at supersonic speeds. The plasma is formed each time the laser sparks or pulses and quickly decays in approximately 10 microseconds (μs). The duration of a laser pulse is typically 10 nanoseconds (ns). Alaser-produced plasma is often referred to as a plasma plume due to its rapid expansion and the continuum of radiation that is produced.

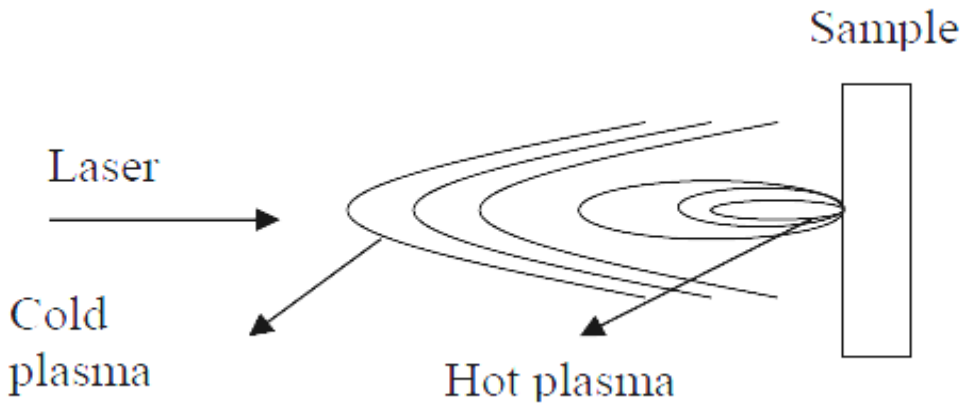

Figure (2.1): Schematic of plasma formation by laser beam

Multi-photon ionization and electron collisions that lead to cascade breakdown are the processes involved in generating a laser-produced plasma. Plasmas are generally described as being partially ionized gases due to the ions and atoms that are formed from the atomization and ionization of the sample (Latresa J. Williamson, 2010).

2.8 Plasma parameter:

Since the derived screened potential should be produced in a statistical way by many charges, we must require that the number of particles inside the Debye sphere be large, $N_D \sim nr^3_D \gg 1$. The parameter $g = 1/N_D$ is often called the plasma

parameter. We see that the condition g « 1 is necessary to ensure that a gas of charged particles behave collectively, thus becoming plasma.

We can arrive at the same parameter in a different way. The average potential energy of the interaction between two charges of the plasma is U ~ q^2/r, where r is the mean distance between the particles. The latter can be estimated from the condition that the there is exactly particle in the sphere with the radius, $\tilde{r}.n\,r^{-3} \sim 1$ so that The average kinetic energy of a plasma particle is nothing but T, $\tilde{r} = n^{-1/3}$ so that:

$$\frac{U}{K} \approx \frac{q^2\, n^{1/3}}{T} \approx \frac{1}{n^{2/3} r_D^2} = g^{2/3} \qquad (2.2)$$

If g « 1, as it should be for a plasma, then the average potential energy is substantially smaller than the average kinetic energy of a particle. In fact, we could expect that since in order that the charges be able to move freely, the interaction with other particles should not be too binding. If U/K « 1, the plasma is said to be ideal, otherwise it is non-ideal (David A. Cremers, Leon J. Radziemski, 2006).

2.8.1. Debye Shielding:

The most important feature of a plasma is its ability to reduce electric fields very Effectively. Plasmas generally do not contain strong electric fields in their rest frames. The shielding of an external electric field from the interior of a plasma can be viewed as a result of high plasma conductivity: plasma current generally flows freely enough to short out interior electric fields. However, it is more useful to consider the shielding as a dielectric phenomena: i.e., it is the polarization of the plasma medium, and the associated redistribution of space charge, which prevents penetration by an external electric field. Not surprisingly, the length-scale

associated with such shielding is the Debye length (Alexander Piel 1987), (Richard Fitzpatrick1, 1998).

Suppose that a quasi-neutral plasma is sufficiently close to thermal equilibrium that its particle densities are distributed according to the Maxwell-Boltzmann law.

$$n_s = n_0 e^{-e_s \Phi / T} \qquad (2.3)$$

Where Φ (r) is the electrostatic potential, and n_0 and T are constant. From $e_i = -e_e = e$, it is clear that quasi-neutrality requires the equilibrium potential to be a constant. Suppose that this equilibrium potential is perturbed, by an amount δ Φ, by a small, localized charge density δρext. The total perturbed charge density is written:

$$\delta\rho = \delta\rho_{ext} + e\,(\delta n_i - \delta n_e) = \delta\rho_{ext} - 2e^2\, n_0 \frac{\delta\emptyset}{T} \qquad (2.4)$$

Thus, Poisson's equation yields:

$$\nabla^2 \delta\emptyset = -\frac{\delta\rho}{\epsilon_0} = -\left(\frac{\delta\rho_{ext} - 2e^2 n_0 \delta\emptyset / T}{\epsilon_0}\right) \qquad (2.5)$$

which reduces to

$$\left(\nabla^2 - \frac{2}{\lambda_D}\right)\delta\emptyset = -\frac{\delta\rho_{ext}}{\epsilon_0} \qquad (2.6)$$

If the perturbing charge density actually consists of a point charge q, located at the origin, so that δρext = q δ(r), then the solution to the above equation is written:

$$\delta\emptyset(r) = \frac{q}{4\pi\epsilon_0 r}\, e^{-\sqrt{2}r/\lambda_D} \qquad (2.7)$$

Clearly, the Coulomb potential of the perturbing point charge q is shielded on distance scales longer than the Debye length by a shielding cloud of approximate radius "D consisting of charge of the opposite sign.

Note that the above argument, by treating n as a continuous function, implicitly assumes that there are many particles in the shielding cloud. Actually, Debye shielding remains statistically significant, and physical, in the opposite limit in which the cloud is barely populated (Richard Fitzpatrick, 1998).

2.8.2. Ionization degree:

A plasma does not have to consist only of electrons, or only of electrons and protons. In other words, neutral particles may well be present. In fact, most laboratory plasmas are only partially ionized. They are obtained by breaking neutral atoms into positively charged ions and negatively charged electrons. The relative number of ions and atoms, $n_i = n_a$, is called the degree of ionization. In general, it depends very much on what is making ionization. However, in the simplest case of the thermodynamic equilibrium the ionization degree should depend only on the temperature. Indeed, the process if ionization-recombination, $a \leftrightarrow i + e$, is a special case of a chemical reaction (from the point of view of thermodynamics and statistical mechanics) (Michael Gedalin, 2008).

2.8.3. Plasma Temperature:

Knowledge of the plasma temperature is vital to understand the dissociation, atomization, ionization, and excitation processes occurring in the plasma and helpful in utilizing the plasma to maximize analytical potential of LIBS. The method most frequently used for determination of excitation temperature of the plasma is the Boltzmann plot method. In this method, the relative intensity of the thermometric species is measured and used for the calculation of the excitation temperature of the plasma by assuming the Local Thermal Equilibrium (LTE)

condition. For LTE to exist in the plasma, the electron density has to be high enough so that the collisional rates exceed the radiative rates.

Plasma temperature can be determined from the ratio of the intensities of:

(1) Neutral to neutral lines.

(2) Ion to neutral lines, usually for the same element.

If the plasma is in local thermal equilibrium then the observed intensity of an excited state, mn is proportional to the density of neutral atoms or ions of this element. The intensity ratio of two lines belonging to the same atomic species is given by (Abdellatif and Imam, 2002).

$$\frac{I_1}{I_2} = \frac{A_1 g_1 \lambda_2 U_2 N_1}{A_1 g_2 \lambda_1 U_1 N_2} \exp[-(\frac{E_1 - E_2}{KT})] \quad (2.8)$$

In the above equation, index 1 refers to the first line and the index 2 to the second line. The two lines belong to the same ionization stage so the partition functions U_1 and U_2 are the same, Thus equation 2.3 can be written as:

$$\frac{I_1}{I_2} = \frac{A_1 g_1 \lambda_2 N_1}{A_2 g_2 \lambda_1 N_2} \exp(\frac{E_1 - E_2}{KT}) \quad (2.9)$$

The accuracy of the temperature determination is better, when the energy difference of the upper terms of the two lines $E_1 – E_2$ is greater. The accuracy may be improved by taking a number of different line pairs and taking the average (Cho et al., 2001). The two lines method can be extended to larger number of lines from the same element and ionized state (Ying et al., 2003).

If the upper state is common and transition terminates to different laser states the intensity of a spectral line is given by (Bekefi, 1997):

$$I = \frac{hcgAN}{4\pi\lambda U} \exp(-E|KT) \quad (2.10)$$

Where in this equation h is Planck's constant, c is the velocity of light, λ is the wavelength of the optical transition between two levels, g is the statistical weight of upper state, E is the energy of the upper state, U is the partition function, K is the Boltzman constant and T is the electrons temperature.

2.9 Lasers for LIBS:

The main properties of laser light which distinguish it from conventional light sources are the intensity, directionality, monochromaticity, and coherence. In addition the laser may operate to emit radiation continuously or it may generate radiation in short pulses. Some lasers can generate radiation with the above mentioned properties and that is tunable over a wide range of wavelengths (David A. Cremers and Leon J. Radziemski, 2006).

Generally pulsed lasers are used in the production of plasmas and also in laser induced breakdown spectroscopy (LIBS). It is possible to generate short duration laser pulses with wavelengths ranging from the infrared to the ultraviolet, with powers of the order of millions of watts. Several billions to trillions of watts and more have been obtained in a pulse from more sophisticated lasers. Such high-power pulses of laser radiation can vaporize metallic and refractory surfaces in a fraction of a second.

It is to be noted that not only the peak power of the laser, but also the ability to deliver the energy to a specific location is of great importance. For LIBS, the power per unit area that can be delivered to the target is more important than the absolute value of the laser power. The power per unit area in the laser beam is termed "irradiance" and is also called "flux" or "flux density." Conventional light sources with kilowatts powers cannot be focused as well as laser radiation and therefore are not capable of producing effects that lasers can (Daived A. cremers, Lion J. Radziemski, 2006).

The next property of laser radiation that is of interest is the directionality of the beam. Laser radiation is confined to a narrow cone of angles which is of the order of a few tenths of a milliradian for gas lasers to a few milliradians for solid state lasers. Because of the narrow divergence angle of laser radiation, it is easy to collect all the radiation with a simple lens. The narrow beam angle also allows focusing of the laser light to a small spot. Therefore the directionality of the beam is an important factor in the ability of lasers to deliver high irradiance to a target. Coherence of the laser is also related to the narrowness of the beam divergence angle and it is indirectly related to the ability of the laser to produce high irradiance. However, coherence is not of primary concern in LIBS. Provided that a certain number of watts per square centimeter are delivered to a surface, the effect will be much the same whether the radiation is coherent or not. The monochromaticity of the laser as such plays very little role as far as plasma production is concerned because it is the power per unit area on the target that matters irrespective of the fact whether the radiation is monochromatic or covers a broad band. In special cases, one may require highly monochromatic laser radiation to probe the plasma using resonance excitation of atomic species (Rosalba Gaudiuso. et al., 2010).

Nd:YAG lasers (flashlamp pumped) are preferred for most LIBS applications because they provide a reliable, compact, and easy to use source of laser pulses of high focused power density. In addition, the fundamental wavelength can be easily shifted to generate pulses with fixed wavelengths ranging from the near IR to the near UV spectral regions. The latter type has been incorporated into compact, person portable instrumentation and a cone penetromter system. These lasers have repetition rates of several kilohertz but produce pulses with maximum energies up to 20 mJ. These have been used to sample solid surfaces such as metals and soils.

These other lasers include the excimer laser (UV wavelengths) and the CO_2 laser (far IR wavelength) that use gas as the lasing medium. In this case an electrical discharge is produced in the gas that pumps the lasing species. The optimum type of laser used for LIBS depends on the application, and the desired laser wavelength (Daived A. cremers, Lion J. Radziemski, 2006).

2.10. Basic LIBS Apparatus:

LIBS is a plasma-based method of atomic emission spectroscopy (AES) that uses originate from the use of a powerful laser pulse to both 'prepare' the target instrumentation similar to that used by other AES methods. The unique characteristics of LIBS sample and then 'excite' the constituent atoms to emit light. Sample preparation results from the action of the focused laser pulse on the target that removes a small mass of the target in the form of atoms and small particles. Coincident with ablation is the formation of a microplasma in the focal volume of the laser pulse that excites the ablated atoms. The plasma continues this excitation after the laser pulse. In addition, small ablated particles are vaporized in the hot plasma and the resulting atoms excited.A typical LIBS apparatus is shown diagrammatically in Figure (2.1).

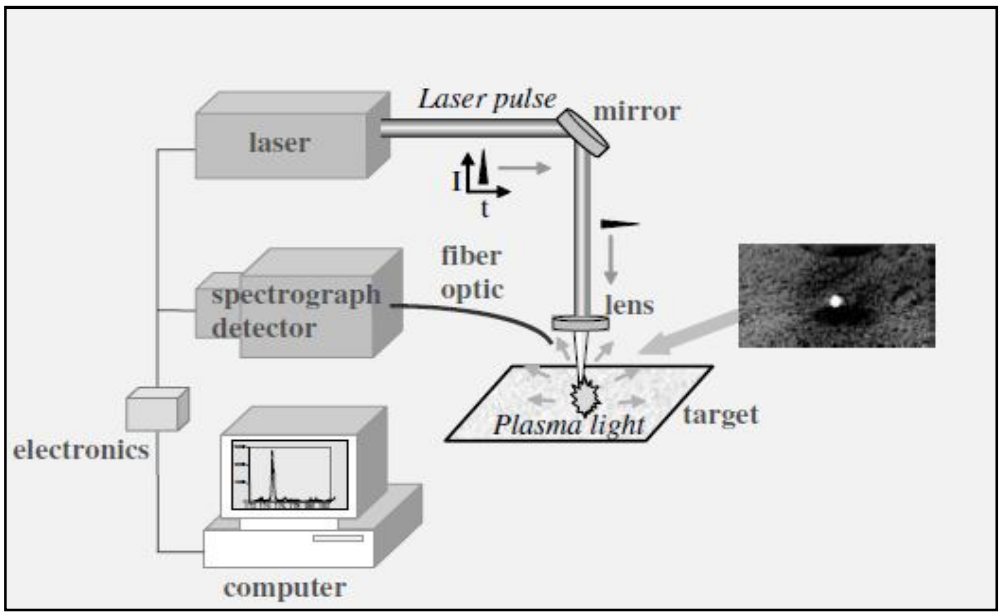

Fig (2.1): A schematic of a simple apparatus for laser-induced breakdown spectroscopy illustrating the principal components.

The main components are:

(1) The pulsed laser that generates the powerful optical pulses used to form the microplasma;

(2) The focusing system of mirror and lens that directs and focuses the laser pulse on the target sample;

(3) Target holder or container (if needed);

(4) The light collection system (lens, mirrors or fiber optic) that collects the spark light and transports the light to the detection system;

(5) Detection system consisting of a method to spectrally filter or disperse the light such as a spectrograph and a detector to record the emission light.

(6) Computer and electronics to gate the detector, fire the laser, and store the spectrum. The basic components of any LIBS system are similar but the component specifications are tailored to the particular application. These specifications include physical parameters such as size, weight, packaging, power and utilities required for operation as well as technical specifications pertaining to operational performance (Daived A. cremers, Lion J. Radziemski, 2006).

The major advantages of LIBS compared to other analytical techniques is that no time-consuming sample preparation is necessary. LIBS uses the plasma generated by a high-energy laser beam to prepare and excite the sample in one step. It has the ability to perform multi-element real-time analysis. Its major disadvantage is that the excitation condition is sensitive to the fluctuation of environmental conditions as well as the laser energy, which can result in poor measurement precision. The small amount of sample material used in LIBS analysis also gives poor sensitivity

for some metals (Fang.Yu Yueh" Jagdish P. Singh, and Hansheng Zhang Missksippi, 2010).

2.11. Applications of LIBS:

2.11.1 Paint and coating identification:

Materials and techniques of paints and coatings require an appropriate verification process to achieve the desired property of the protective finishing. The organic coating involves a multi-step process in which the quality of the metal finish required for an industrial product would determine the number and the type of steps in a given process (Prefetti, B. M., 1994). These multi-step coating processes include the selection and composition verification of substrates, surface cleaning, surface pre-treatment, primer, topcoat, and the application of paint curing methods. The paint formulation is a mixture of multi-ingredients, composing: resins, solvents, pigments, fillers, corrosion inhibitors, and other rheological additives. The organic coating in metal finishing practice is extremely complex. The complexities of paint compositions, paint types, and painting processes make their chemical analysis very difficult. In spite of some elemental analysis methods that have been well established for the general purpose in chemistry, the determination of metallic components in paint has been relied on the indirect analytical methods. For example, the metallic zinc dust in the Zn-rich epoxy primer was determined by differential scanning calorimetry (DSC) (Weldon, D. G., Carl, B. M., 1997). The DSC method measured the apparent heat of fusion of the paint sample, and compared this measured value to the standard value of pure zinc as an indirect measurement of zinc composition in paint. Infrared absorption spectroscopy is useful sometimes for the composition analysis if the paint ingredients contain any

specific functional groups which are spectroscopically active (stamenkovic, J.et al., 2004), such as the isocyanate group in the urethane. The direct analysis of these functional groups may be possible only if the paint sample is uncured, and contained a relatively simple composition. In practice, there is no direct way for identifying a cured paint film. Once the paint, e.g. epoxy or urethane, is applied and fully cured, no more epoxy or isocyano functional group would remain in the paint film. Even though, the researchers have attempted to characterize the fully cured paint products by identifying the hydroxyl or amino groups, and use them for differentiating the epoxy paint or urethane paint. The results are generally inconclusive because the majority of other cured paints also have those functional groups as reaction products. The LIBS technique described in this section shows the capability of coating identification at the specimen surface (Kim T. et al., 2007)

2.11.3 Organic and biomaterial screening:

Biomaterial application has two areas depending on the analytical goal. The first goal is the analysis of metallic component in the biomaterial. The conventional elements like Na, K, Ca, Mg are included in plant, wood, grain, tissue and bio-remains. Their analysis is similar to other solid samples except those samples include high level of carbon compound. The second application of biomaterial is characterization of biomaterial itself. Breakdown spectrum from LIBS can have information of specific sample group. One of the researches has been made for classification of bacterial strains by major components analysis with LIBS (Kim T. et al., 2007)

2.11.3 Application of LIBS for metallic component in aqueous solution:

LIBS has the capabilities to perform rapid analysis of solid and liquid samples. It can significantly reduce the time and costs associated with the sample preparation and therefore a useful technique for environmental monitoring and other related

applications (Lee *et al.*, 2000, Hussain *et al.*, 2008). LIBS has been applied to many environmental situations.

As mentioned at the LIBS property, solid samples are most convenient and strong LIBS signal. Liquid or gas samples need more specific optical arrangement to generate breakdown and emitting light collection. There are several ideas to overcome the sampling difficulty of gas and liquid samples. One of the publications here is a typical sample type conversion from liquid sample to solid with concentrating effect. Ion-exchange resins are conventional substances used to capture metal ions and hold them in the solid resin matrix. Chemically activated microporous membranes functionalized with polycarboxylic acid are typically. Employed (Hestekin, J.; et al, 2000). The matrix encapsulation technique has been applied to collect trace metals from water, and converting metal ions to a solid form. The pre-concentration of analyte from a liquid sample into the ion exchange membrane was extensively studied for LIBS measurement by Schmidt and Goode (Schmidt, N., Goode, S., 2002).

2.12. LIBS for pollution detection in environment:

The application of LIBS to environmental monitoring has drawn significant attention. LIBS has been used to detect toxic metals in soil and paint, and has been explored as a multimetal continuous emission monitor (CEM).

There are a few reports on the application of LIBS to detect radioactive species. LIBS has also being used to measure the composition of molten metals and glasses (Fang.Yu Yueh" Jagdish P. Singh, and Hansheng Zhang, 2000).

Due to rapid industrial growth, environmental pollution has increased tremendously over the years, especially the contamination of soil and ground water with heavy metals such as chromium, lead, copper, arsenic, nickel, beryllium, antimony, zinc, magnesium, aluminum, cobalt etc. These metals, are toxic even at

low concentrations, may find their way into the human body via inhalation, ingestion, and skin absorption. If accumulation of the heavy metal ions in the body tissues is faster than the body's detoxification, a gradual buildup of these toxins will occur. Long and even short term exposure to measurable quantities of various metals such as lead, mercury, copper, nickel, arsenic, beryllium, molybdenum, zinc, chromium and antimony can lead to long term health problems and can cause irreversible damage.

The exposure to excessive concentrations of cadmium and mercury has produced adverse health effects in public. In addition, some of these elements may have detrimental effects upon crop growth and yield. They may also have adverse effects on ecosystem if their proper detection, analysis, disposal and dispersal are not regulated. These metals can enter in to human body by contact to open lying contaminated sludge, irrigating crop with untreated waste water, chemicals, industrial waste and effluents. The exposure to heavy metals is a serious growing problem throughout the world. The incidences of human exposure to these metals have risen dramatically in the last 10 years (Fergusson, 1990; Islam *et al*., 2007).

Keeping in view the above mentioned harmful effects of these metals, there is a need for rapid and precise determination of the concentration of contaminants, in the environment. The interest for the development of new analytical techniques has increased in the recent years to assess and monitor the extent of environmental contamination in water resources, soil, and waste disposal sites. Most of the available methods are generally expensive or time-consuming due to sample preparation, require special reagents/chemicals and are not cost effective (Rai *et al*.,2001; Uhl *et al*., 2001; Russell *et al*., 2005).

A significant part of the anthropogenic emissions of heavy metals ends up in wastewater. Major industrial sources include surface treatment processes with elements such as Cd, Pb, Mn, Cu, Zn, Cr, Hg, As, Fe and Ni, as well as industrial

products that, at the end of their life, are discharged in wastes. Major urban inputs to sewage water include household effluents, drainage water, business effluents (e.g. car washes, dental uses, other enterprises, etc.), atmospheric deposition, and traffic related emissions (vehicle exhaust, brake linings, tires, asphalt wear, gasoline/oil leakage, etc.) transported with storm water into the sewerage system. For most applications of heavy metals, the applications are estimated to be the same in nearly all countries, but the consumption pattern may be different. For some applications which during the last decade has been phased out in some countries, there may, however, today be significant differences in uses.

Most common sources of heavy metals to waste and/or waste water are;

(i) Mining and extraction; by mining and extraction a part of the heavy metals will end up in tailings and other waste products. A significant part of the turnover of the four heavy metals with mining waste actually concerns the presence of the heavy metals in waste from extraction of other metals like zinc, copper and nickel. It should, however, be kept in mind that mining waste is generated independent of the subsequent application of the heavy metal.

(ii) Primary smelting and processing; a minor part of the heavy metals will end up in waste from the further processing of the metals.

(iii) Use phase; a small part of the heavy metals may be lost from the products during use by corrosion and wear. The lost material may be discharged to the environment or end up in solid waste either as dust or indirectly via sewage sludge.

(iv) Waste disposal; the main part of the heavy metals will still be present when the discarded products are disposed off. The heavy metals will either be collected for recycling or disposed of to municipal solid waste incinerators (MSWI) or landfills or liquid waste. A minor part will be disposed of as chemical waste and recycled or landfilled via chemical waste treatment.

(v) Vulconic erruptions.

(vi) Fossil fuel combustion.

(vii) Agriculture.

(viii) Aerosions.

(ix) Metallurgical industries. Actually metal pollutants are neither generated nor compleletely eliminated; they are only transferred from one source to another. Their chemical forms may be changed or they are collected and immobilized not to reach the human, animals or plants (Baysal et al., 2013).

In LIBS analysis of liquid samples, one requires high pulse energy of the incident laser beam to generate plasma and to excite the sample species into ionic and neutral atomic transitions. In order to study the effect of the laser energy on the line emission intensity, we recorded the plasma emission spectra of waste water sample at different laser energies (Hussain T., gondal M.A., 2008). Figure (2.2) bellow showed one of the LIBS setup which was used for liquid analysis.

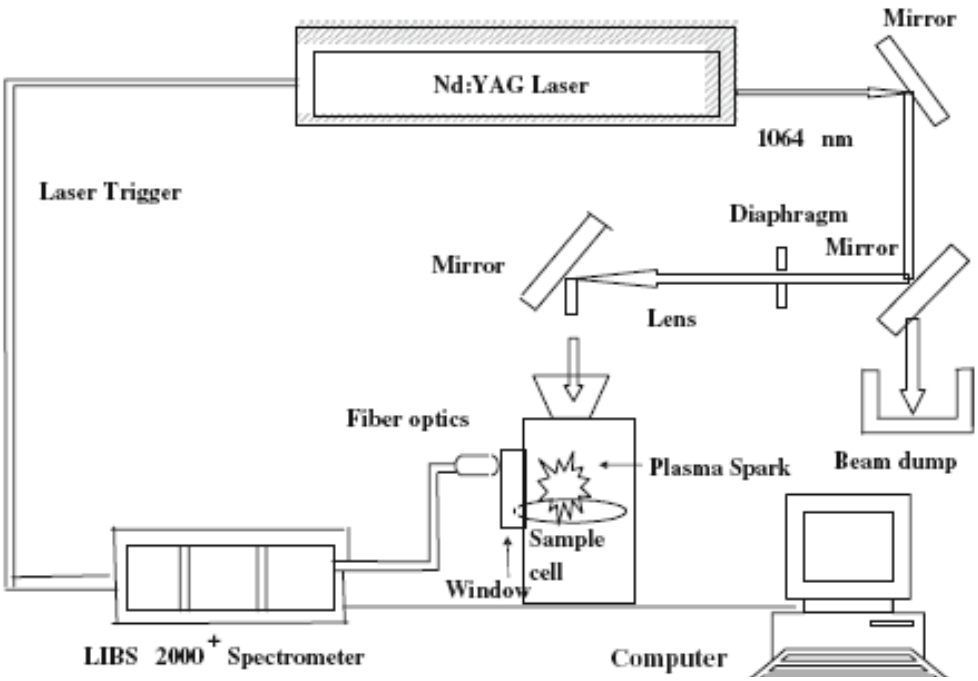

Fig (2.2): The experimental setup of LIBS for liquid sample

2.13 Toxicity of heavy metals:

The Heavy Metals test kits are designed especially to detect the presence of toxic heavy metals in the body using urine or saliva. They can also be used to detect heavy metals in most clear liquid medium. It is important to check the presence of heavy metals because they are the main cause of excessive free radical activity, which can cause damage to the healthy state of the body including depleting the body'simmune system. The Heavy Metals Test kits can also be used to confirm the presence of metals/minerals in food such as iron in rice, etc.

Toxic heavy metals can cause the following health problems:

long term exposure to cadmium is associated with renal dysfunction. Cadmium is biopersistent and once absorbed remains resident for many years. High exposure can lead to obstructive lung diseases and has been linked to lung cancer. Cadmium may also cause bone defects in humans and animals. The average daily intake for humans is estimated as 0.15µg from air and 1µg from water; low exposure to chromium can irritage the skin and cause ulceration. Long term exposure can cause kidney and liver damage. It can also cause damage to circulatory and nerve tissues; high doses of copper can cause anemia, liver and kidney damage, and stomach and intestinal irritation. People with Wilson's disease are at greater risk for health effects from overexposure to copper; exposure to lead can lead to a wide range of biological defects in human depending on duration and level of exposure. The developing feotus and infants are far more sensitive than adults. High exposure can cause problems in the synthesis of haemoglobins, damage to the kidneys, gastrointestinal tract, joints, reproductive system and the nervous system. Studies have suggested that exposure to lead can cause up to a loss of 2 IQ points; inorganic mercury poisoning is associated with tremours, gingivitis and/or minor pyschological changes together with spontaneous abortion and congenital

malformation. Monomethylmercury causes damage to the brain and the central nervous system while fetal and post-natal exposure have given rise to abortion, congenital malformation and development changes in young children; excessive amounts of nickel can be mildly toxic. Long term exposure can cause decreased body weight, heart and liver damage andskin irritation; exposure to high levels of arsenic can cause death. All types of arsenic exposure can cause kidney and liver damage and in the most severe exposure there is erythrocyte hemolysis;

manganese is known to block calcium channels and with chronic exposure results in CNS dopamine depletion. This duplicates almost all of the symptomology of Parkinson's Disease.

aluminium toxicity is associated with the development of bone disorders including fractures, osteopenia and osteomalacia (http://heavymetalest.us.detox.php).

The more commonly encountered toxic heavy metals are Arsenic, Lead, Mercury, admium, Iron, Aluminium. Heavy metal toxicity represents an uncommon, yet clinically significant, medical condition. If unrecognized or inappropriately treated, heavy metal toxicity can result in significant morbidity and mortality. The most common heavy metals implicated in acute and/or chronic conditions include lead, arsenic, and mercury (www.piacton.com).

2.14 Literature review:

Walid Tawfig, Y. Mohamed in 2007 used Calibration free laser-induced breakdown spectroscopy (LIBS) to identify seawater salinity. They used it as a remote sensing system to analyze seawater samples and to identify their salinities without ordinary calibration curves. The plasma is generated by focusing a pulsed Nd:YAG laser on the seawater surface in air at atmospheric pressure. Such plasma emission spectrum was collected using wide band fused-silica optical fiber of one-meter length connected to a portable Echelle spectrometer with intensified CCD camera. They characterized Spectroscopic analysis of plasma evolution of laser

produced plasmas in terms of their spectra, electron density and electron temperature assuming the local thermodynamic equilibrium (LTE) and optically thin plasma conditions. Three elements (Na, Ca and Mg) were determined in the obtained spectra to identify the salinity of seawater samples. They determined electron temperature T_e and density N_e using the emission intensity and Stark broadening. The obtained values of T_e and N_e for natural seawater sample (salinity 3.753%) were 11580 K ± 0.35% and 3.33×10^{18} cm^{-3} ± 14.3%. These values exhibit a significant change only if the matrix changes (i.e., the salinity changes). On the other hand, no significant difference was obtained if T_e and N_e were determined using any of the three elements (Na, Ca and Mg) in the same matrix. It is concluded that T_e and N_e represent a fingerprint plasma characterization for a given seawater sample and its salinity could be identified using only one element without need to analyze the rest of elements in the seawater matrix. The obtained results indicated that it was possible to improve the exploitation of LIBS in the remote on-line environmental monitoring, by following up only a single element as a marker to identify the seawater matrix composition and salinity without need to analyze that matrix which saves a lot of time and efforts.

Monica Simileanu, Roxana Radvan, Niculae Puscas in 2010 used LIBS setup for identification of metals underwater. The results of the underwater LIBS analysis of the spectral lines prove that this photonic technique is more than suitable for underwater investigations, providing reliable and accurate information, without requiring the removing the object from its aqueous environment. The information provided by the underwater spectra is more than enough for the interpretation and discrimination of the elemental compound. It is very clear, as stated before, that the double pulse LIBS technique is the one that gives the most interesting and clear results after the analyzes of the spectra.

In 2009, Y. Godal, M.T. Taschuk, S.L. Lui, Y.Y. Tsui and R. Fedosejevs have demonstrated that by the resonant dual-pulse technique the sensitivity of the LIBS can be increased with orders in magnitude reduction in the ablation pulse energy, which makes the realization of a field portable spectrometer more realistic. Even though in the 100 ppb range for Pb significant improvements can be made. Possible approaches are to increase the resonant pulse energy, improve the collection optics and integrate more shots using higher repetition rate lasers. In addition, a more sophisticated analysis of the signal such as noise spike rejection and an emission line fitting approach may be employed. A 2D map of a fingerprint on a Si wafer has been successfully acquired using 5 μJ pulses, demonstrating that fiber or microchip lasers with kHz repetition rates could be used as the excitation source for a portable μLIBS fingerprint scanner. These μLIBS techniques can also be applied to microfluidic Lab on Chip applications for the measurement of elemental content of micro specimens of fluids. Considerable work is still required in order to determine the optimum configuration and limit of detection obtainable for such systems.

Boudjemai, S, Gasim, et. al., in 2004 they reported from experimental results on the temporal characteristics of laser spark emission spectra. Sparks were generated in water by the focused beam of a Q-switched Nd:YAG laser Na and Cu aqueous solutions exhibited fluorescence signal on the decaying edge of plasma emission at their respective characteristic resonance lines. Potential of the laser plasma spectroscopy for in-situ pollution monitoring in natural and wastewater is briefly discussed.

In 2011, X. Fang · S.R. Ahmad proved that laser-induced breakdown spectroscopy allows detection of mercury in aqueous matrix at a ppb level of concentration using pre-concentration of target species. Pre-concentration has been most effectively carried out on a metal plate by electrolysis before subjecting the plate to LIBS

analysis. A pre-concentration factor of ~180 for the mercury determination in triple-distilled water was achieved. This has greatly increased the capability and applicability of LIBS for trace metal detection in water. Such improvement has been achieved from its previous status where mercury detection in water at concentrations of even a few thousands ppm was difficult by direct LIBS probe in water bulk medium and for solid sample the reported limit of detection for mercury was just above ppm level. Their study is an initial evaluation of the pre-concentration method as assistance for LIBS. The further investigation is being undertaken to optimize the technique to even further lower limit of detection and improve the sensitivity and reproducibility of LIBS for the detection of heavy metals including mercury in water. Possible industrial applications of LIBS for aqueous samples with such pre-concentration method are also being explored.

Qassem I, et. al., in 2012 reported that a LIBS-based bacterial identification could be successfully applied to identify pathogens in a clinical specimen. The issue of mixed samples has once again been addressed with mixtures prepared from two closely related bacteria (E. coli and E. cloacae) using clinically relevant and realistic mixing fractions. Their work was intended to represent situations of clinical infections with the presence of additional background or contaminant bacteria. To simulate the use of a LIBS-based test to diagnose urinary tract infections, cells of S. epidermidis were spiked into sterile urine samples and the bacteria were harvested from these samples with no other preparation or washing. Using a discriminant function analysis model that contained spectra from S. epidermidis cells harvested from water as well as two other staphylococci species, the urine-harvested samples were identified with 100% accuracy. No spectrum, used to construct the model, was obtained from cells obtained from a urine sample. A 669-spectrum library composed of spectra from five bacterial genera and 13 distinct taxonomic groups was compiled and tested using external validation

techniques where the model did not contain any spectra from samples acquired at the same time.

Little difference was observed between the five-class model and the 13-class model. Truth tables constructed from the external validation of the five genus model yielded sensitivities of approximately 85% and specificities above 95%. These external validation tests were compared to LOO cross-validation tests and, as expected, an artificially high accuracy was observed in the LOO tests. Last, the use of sequential classification testing was investigated by identifying closely related E. coli and E. cloacae spectra using first the five-genus model spectral library and then a more targeted model that contained only E. coli and E. cloacae spectra. The improvement in accuracy obtained by using the more targeted model demonstrated the utility of using sequential testing to "filter" unknown spectra as they are tested, first through a "coarse" (perhaps genus-level) model and then through a more "fine" species-level (or similar) model to eventually obtain an accurate identification at the desired level. This simple addition of sequential testing can be easily implemented with little to no increase in complexity or time required.

T. Hussain AE. M. A. Gondal in 2007 developed locally Laser Induced Breakdown Spectroscopy (LIBS) System for determination of toxic metals in liquid samples and the system was tested for analysis of waste water collected from dairy products processing plant. The plasma was generated by focusing a pulsed Nd: YAG laser at 1064 nm on waste water samples. Optimal experimental conditions were evaluated for improving the sensitivity of their LIBS system through parametric dependence investigations. The Laser-Induced Breakdown Spectroscopy (LIBS) results were then compared with the results obtained using standard analytical technique such as Inductively Coupled Plasma Emission Spectroscopy (ICP). The evaluation of

the potential and capabilities of LIBS was found as a rapid tool for liquid sample analysis.

In 2009, Matthew Weidman1, Matthieu Baudelet, Santiago Palanco, Michael Sigman, Paul J. Dagdigian, Martin Richardson used double pulse irradiation with Nd:YAG and CO_2 lasers as Laser-induced breakdown spectroscopy (LIBS) was applied to the analysis of a polystyrene film on a silicon substrate. An enhanced emission signal, compared to single-pulse LIBS using a Nd:YAG laser, was observed from atomic carbon, as well as enhanced molecular emission from C_2 and CN. This double-pulse technique was further applied to 2,4,6-trinitrotoluene residues, and enhanced LIBS signals for both atomic carbon and molecular CN emission were observed; however, no molecular C_2 emission was detected.

Anna P. M. Michel, Marion Lawrence-Snyder, S. Michael Angel, and Alan D. Chave in 2007 used Laser-induced breakdown spectroscopy as a promising in situ technique for oceanography. Laboratory investigations on the feasibility of using LIBS to detect analytes in bulk liquids at oceanic pressures were carried out. LIBS was successfully used to detect dissolved Na, Mn, Ca, K, and Li at pressures up to $2.76 * 10^7$ Pa. The effects of pressure, laser-pulse energy, interpulse delay, gate delay, temperature, and NaCl concentration on the LIBS signal were examined. An optimal range of laser-pulse energies was found to exist for analyte detection in bulk aqueous solutions at both low and high pressures. No pressure effect was seen on the emission intensity for Ca and Na, and an increase in emission intensity with increased pressure was seen for Mn. Using the dual-pulse technique for several analytes, a very short interpulse delay resulted in the greatest emission intensity. The presence of NaCl enhanced the emission intensity for Ca, but had no effect on peak intensity of Mn or K. Overall, increased pressure, the addition of NaCl to a solution, and temperature did not

inhibit detection of analytes in solution and sometimes even enhanced the ability to detect the analytes. The results suggest that LIBS is a viable chemical sensing method for in situ analyte detection in high-pressure environments such as the deep ocean.

1n 2014, Peichao Zheng, et. Al. determined trace mercury in an aqueous solution using laser-induced breakdown spectroscopy with the assistance of a solution cathode glow discharge (SCGD) system. They converted the aqueous solution to the gas phase using a high voltage DC discharge, and then the generated mercury vapor was cooled by a gas–liquid separator to improve the concentration of the mercury. Finally, a 1064 nm wavelength Nd:YAG laser was used to produce the plasma. Characteristic spectral line of HgI 253.65 nm was selected for the analysis, under the optimal conditions of LIBS, to investigate the influences of the acid anion, the discharge current, the sample flow rate and the carrier gas flow rate. The temporal behavior of the electron temperature and electron number density were also investigated; From the results, they showed that the electron temperature decreases from about 10900 K to 8800 K with a delay time from 200 ns to 6 μs and that the electron number density is in the orders of 10^{17} and 10^{18} cm^{-3}, and decreases with delay time. They evaluated the analytical performance of this method under optimized conditions, and a calibration curve of Hg was plotted based on the different concentrations measurement results, and the detection limit (LOD) of Hg was calculated to be 0.36 mg L^{-1}. By this experimental configuration, the detection limit and sensitivity of Hg are improved to some extent. This method provides an alternative analytical method for the measurement of trace mercury in water.

Qi Shi, et.al. in 2014 combined nano-channel material with laser induced breakdown spectroscopy (LIBS) to achieve sensitive and quick detection of metal ions in liquid samples. A 3D anodic aluminum oxide porous membrane (AAOPM)

was selected as a novel substrate for the first time, which showed excellent potential for liquid analysis. It is worth mentioning that the LIBS signal of the target elements in aqueous solution dropped on the 3D AAOPM was increased by up to 19 times in comparison with that on the tablet sample made of aluminium oxide powder. The attractive results were mainly attributed to the peculiar structure of the 3D AAOPM. Firstly, an abundant strong coordination metal–oxygen bond between hydroxyl groups and metal ions existed on the surface of the novel substrate. Secondly, the extremely high aspect ratio of the 3D AAOPM could supply a much larger contact area between the matrix and analytes. Thirdly, the special nano-channel distribution could make efficient coupling of a laser beam with the materials. Finally, the sample pervasion and volatilization could be finished within a very short time because of the micrometer level thickness and porosity of the 3D AAOPM. The calibration curves with linearity ranges (1–100 μg mL^{-1}) and good linearity (*R* squared better than 0.983 for all of the four target elements) were established, and the limits of detection (LODs) obtained were 0.18 μg mL^{-1}, 0.12 μg mL^{-1}, 0.081 μg mL^{-1}, and 0.11 μg mL^{-1} for Cu^{2+}, Ag^{+}, Pb^{2+}, and Cr^{3+}, respectively. In real sample analyses, the recoveries of three elements at different concentration levels were all in the range of 92.5–107.4%, with the relative standard deviations of parallel samples around 10.0%. This novel method showed a fast, simple and super sensitive monitoring tool for liquid sample analysis compared with the traditional LIBS method.

In 2013 Tomoko Takahashi, et. al. used Long-Pulse Laser-Induced Breakdown Spectroscopy for analysis of the composition of rock and sediment samples submerged in seawater to investigate the application of Laser-Induced Breakdown Spectroscopy to qualitatively analyze the composition of various seafloor rock samples in seawater. They achieved well-resolved emission spectra of submerged samples by using a long laser pulse of duration 250 ns. They found that the main

elements in each rock sample could be successfully identified both in pure water and in seawater. When comparing the measurements made in pure water and in seawater, some effects of the seawater could be seen. The results suggested that long-pulse LIBS may be applicable for in situ, multi-element chemical analysis of sediments and rocks in the marine environment.

Chapter Three

Materials and Methods

Chapter three

Materials and Methods

3.1. Introduction:

In the dairy product industry, there is a need for an analytical technique to be able for on line measurements of heavy metals and other trace elements in waste water coming from different processes involved. The amount of waste water generated by dairy industrial plant is of huge amount and it can have hazardous effects on environment.

Most of the dairy plants produce pasteurized milk, cream, buttermilk, chocolate milk, ice cream mix, and fruit juice drinks. During the manufacturing process of dairy products, raw milk processing is one of the important processes.

Raw milk is pumped to centrifuge clarifier where undesirable solids in the milk are removed and the waste from the clarifier is collected and can be reused as fertilizer. In pasteurized milk processing, waste water is disposed of to the municipal sewerage system. During the washing process, milk remaining in the presses could be contaminated with the chemicals used for the processing and detergents used for cleaning. This contaminated milk is also disposed of in the municipal sewerage system. Similarly, the skim milk from storage tank is pumped to a processing tank.

The instrumentation of LIBS is relatively simple as compared to other analytical techniques such as mass spectrometry, laser-induced fluorescence, inductively coupled plasma-atomic emission spectrometry (ICP-AES) etc.

This chapter demonstrates and explains the experimental setup, materials, instruments and experimental procedure used during this work for the investigation of elements in different types of waste water collected from diary product plant and

its concentrations. The LIBS spectrometer was tested for the analysis of waste water from dairy product plant.

3.2 The samples:

The dairy plant wastewater samples were collected from a local plant located in Khartoum city, Sudan in plastic bottles. All bottles were thoroughly washed with Distilled water. Five industrial wastewater samples were collected from different dairy product plants and investigated in this work.

3. 3 Collection of samples:

The waste water samples were collected in plastic bottles during the peak working hours of dairy syringes manufacturing plants. The plastic bottles were sterilized and washed with distilled water before sampling to avoid any type of contamination.

3.4 The experimental setup:

The experimental components used in this work are shown in figure (3.1) and schematically depicted in Fig (3.2).

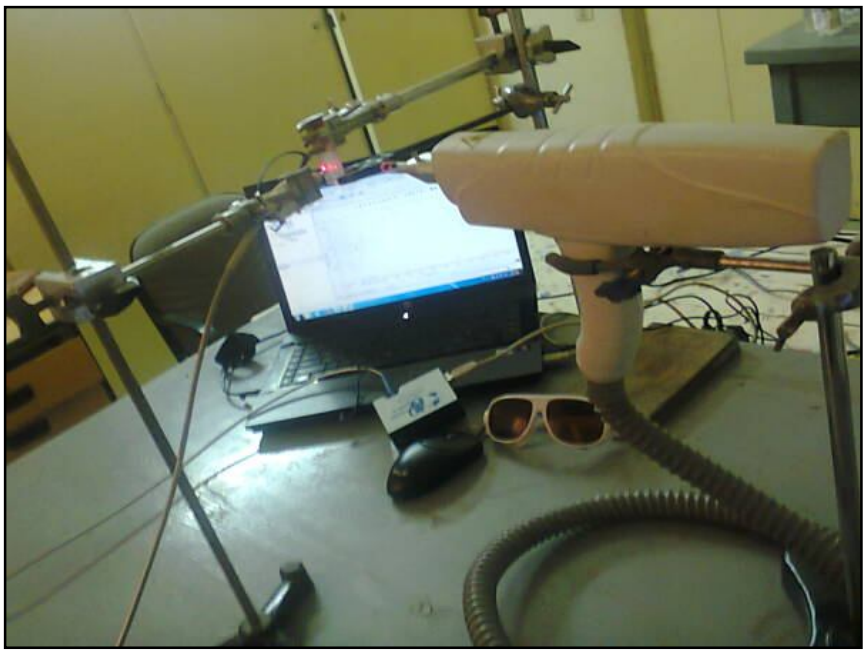

Fig. (3.1): The experimental setup

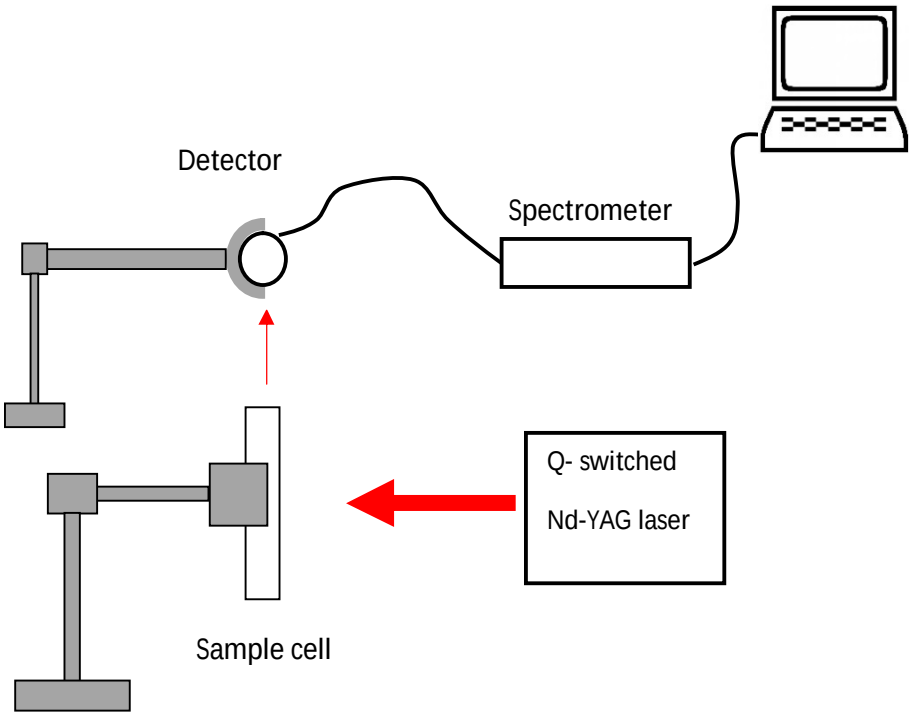

Fig (3.2): Schematic diagram of the setup

It was consisted of:

3.4.1 The laser:

Nd - YAG Laser System structure is mainly consisted of the following units Power Supply, Laser Hand piece, Control Union and Cooling System. The power supply is assembled in the main case. The specifications of the Nd – YAG laser was used in this work are listed in table (3.1).

Table (3.1) laser specifications:

component	Specifications
Company	Shanghai Apolo Medical Technology Co., Ltd China
Power Supply:	~230V, 50/60Hz
Model	HS-220
Laser Type	Q switched Nd - YAG Laser
Laser wavelength:	1064nm & 532nm
Weight	20 kg
Pulse width:	10ns
Repeat frequency	1、2、3、4、5HZ
Lead light method	directly export laser
The light spot diameter	2~8mm
Power supply	90-130V, 50Hz/60Hz or 200-260v, 50Hz
Environment temperature:	5˚C～40˚C
Relative humidity:	80%
Cooling system	the water-cooling + the air cooling inside. System device overview

Front view of the laser is shown in fig (3.3):

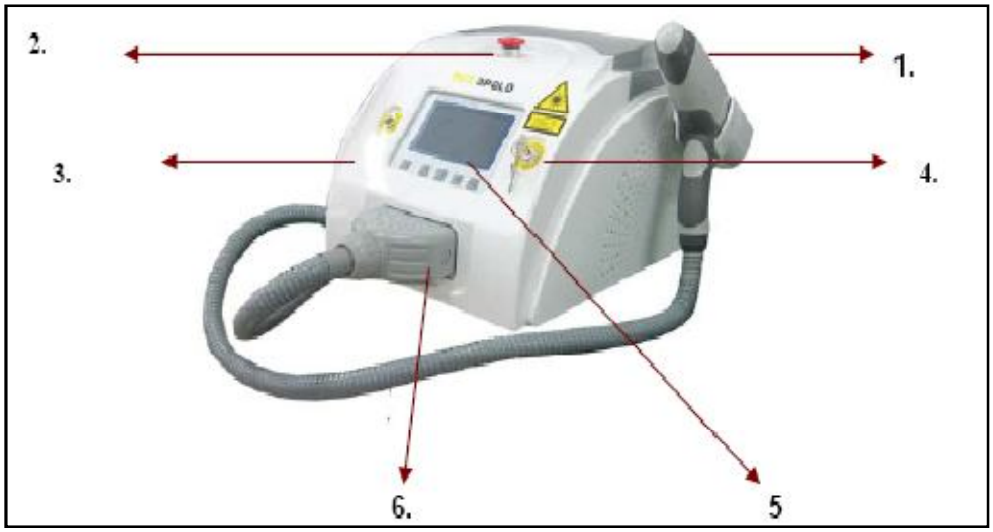

Fig (3.3): Front view of Nd: YAG Laser s System

1 .Laser hand piece

2. Emergency switch

3. Main host

4. Key switch

5. LCD control panel

6. Handpiece Connector.

Emergency switch: While appearing the urgent circumstance, pressing it, the power will be cut off. Revolving the switch according to arrowhead direction, the power supply renew.

Key switch: Whole switch of power

SIMMER key：At the "Operation Interface-SIMM", this key can make the instrument enter the situation from S (Standby) to R (Ready) mode，the xenon flash lamp is triggered for and may go further to work mode. Pressing "SIMMER" key again, the system will escape from ready to standby and the xenon flash lamp is off.

MENU key: At the "Operation interface-FREQ", this key can set the frequency of each second from 1 to 5 Hz.

Up key：At the "Operation interface-PWR+", this key system enters the interface of power energy adjustment; Press again, can increase the power energy

Down key：At the "Operation interface-PWR-", this key, system enters interface of power energy adjustment; Press again, can decrease the power energy.

Enter key：At the "Operation interface-SET", this key, can make the machine select Laser frequency 1064nm or 532nm when it is on the standby mode. Or when the system is ready on "Operation interface-R", pressing this key enters the system to "W" work mode. The work appearance, press the foot switch, the Laser output

for treatment. Or when the system is in working mode on “Operation interface-W”, press this key the system will escape from work to ready mode. Press Simmer key again; the system will enter to standby mode.

This laser source was used for plasma generation with different Pulse Energies (30, 60, 80, 100) mJ and 20 pulses. This type of the laser is the most widely used due to its reliability to produce powerful laser pulses, particularly because it is Q-switched. The laser pulse energies required to generate plasma depend on many factors including properties such as (energy, mode quality, wavelength, and pulse length) and the material (density of material).

3.4.2 **A glass cuvette cell:** was used to put the samples in it with diminutions 3cm x 1cm x 3cm.

3.4.3 **Optical System:** consisted of mirrors and concave lenses.

3.4.4 **Detection System,** consist of:

(i) The spectrometer: The spectrometer used in this work was Ocean Optics LIBS 4000+ Its model USB4-UV/VIS, with dimensions (in mm): 89.1 x 63.3 x 3.4.4, Fig (3.5) shows the internal components of this spectrometer.

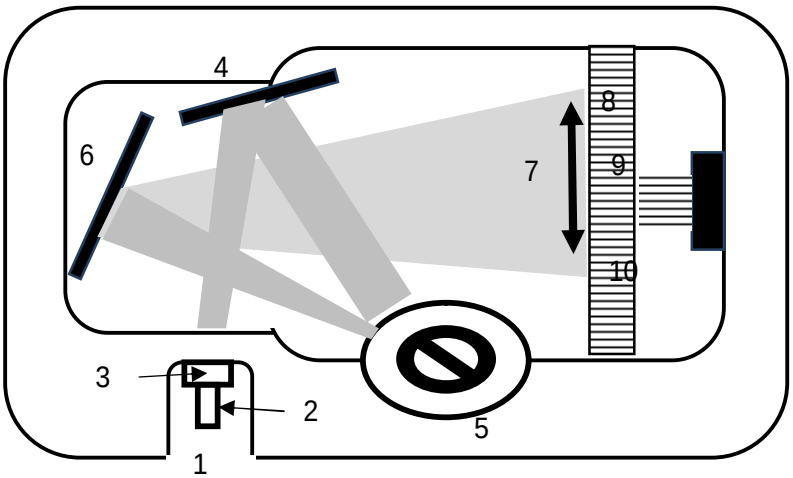

Fig (3.4): The USB4000 Spectrometer

It was supplied from ocean optics with the following specifications: a 16-bit A/D, four triggering options, a dark-level correction during temperature changes, and a 22-pin connector with eight users programmable GPIOs. The USB4000 interfaces to computer with Windows operating system. The modular USB4000 is responsive from 200-850 nm and it can be configured with various Ocean Optics optical bench accessories, light sources and sampling optics to create application-specific systems for thousands of absorbance, reflection and emission applications.

The USB4000 Spectrometer is distinguished by its enhanced electronics: 16-bit A/D resolution with auto nulling feature (an enhanced electrical dark-signal correction); EEPROM storage of calibration coefficients for simple spectrometer start-up; 8 programmable GPIO signals for controlling peripheral devices; and an electronic shutter for spectrometer integration times as fast as 3.8 milliseconds, a handy feature to prevent detector saturation. In addition, the USB4000 has signal to noise of 300:1 and optical resolution (FWHM) ranging from 0.03-8.4 nm (depending on the grating and entrance aperture selection). The detector was Toshiba TCD1304AP linear CCD array detector range: (200-850) nm, with 3648 pixels of size (8 μm x 200 μm) and Pixel well depth about 100,000 electrons with sensitivity: 130 photons/count at 400 nm; 60 photons/count at 600 nm. The grating of the spectrometer type is 600 lines blazed at 300 nm.

The USB4000 interfaces to a computer via USB 2.0. Data unique to each spectrometer and is programmed into a memory chip on the USB4000; spectrasuite spectroscopy operating software reads these values for easy setup and hot swapping among computers, whether they run on Linux, Mac or Windows

operating systems. When connected to a computer via USB, the USB4000 draws its power from the computer.

1- **SMA 905 Connector** Light from a fiber enters the optical bench through the SMA 905 Connector. The SMA 905 bulkhead provides a precise locus for the end of the optical fiber, fixed slit, absorbance filter and fiber clad mode aperture.
2- **Fixed Entrance Slit**: Light passes through the installed slit, which acts as the entrance aperture. The slit is fixed in the SMA 905 bulkhead to sit against the end of a fiber.
3- **Long pass Absorbing Filter:** An absorbance filter is installed between the slit and the clad mode aperture in the SMA 905 bulkhead. The filter is used to block second- and third order effects or to balance color.
4- **Collimating Mirror:** is matched to the 0.22 numerical aperture of the optical fiber. Light reflects from this mirror, as a collimated beam, toward the grating. One can install a standard mirror or a UV absorbing SAG+ mirror.
5- **Grating & Wavelength Range:** installed on a platform that rotate to select the starting wavelength that have specified. Then the grating permanently fixed in place to eliminate mechanical shifts or drift.
6- **Focusing Mirror:** This mirror focuses first-order spectra on the detector plane. Both the collimating and focusing mirrors are made in-house to guarantee the highest reflectance and the lowest stray light possible.
7- **L4 Detector Collection Lens:** This cylindrical lens, made in-house to ensure aberration-free performance, is fixed to the detector to focus the light from the tall slit onto the shorter detector elements. It increases light-collection efficiency.

8- **Detector** There are 3648-element Toshiba TCD1304AP linear CCD array detector. Each pixel responds to the wavelength of light that strikes it. Electronics bring the complete spectrum to the software.

9- **OFLV Variable Long pass Order-sorting Filter:** the proprietary filters precisely block second- and third-order light from reaching specific detector elements

10- **UV4 Detector Upgrade:** The detector's standard BK7 window is replaced with a quartz window to enhance the performance of the spectrometer for applications <340 nm.

(ii) The optical fiber:

The optical fiber used to collect spectra was supplied by ocean optics. It is type UV - VIS model QP600-2-UV-BX 600 μm diameter AND two meter length silica core. Surrounding the core is a doped-fluorine silica cladding. A buffer material is then applied. A buffer coats the core and cladding , strengthens the fiber and reduces stray light even further. In most assemblies polyimide is used as the buffer; other assemblies use aluminum or acrylate. Then a jacketing is applied over the core, cladding and buffer to protect the fiber and provide strain relief as shown in Figure (3.6). For off-the-shelf Premium-grade "Q" Optical Fiber Assemblies, the standard jacketing is stainless steel.

Precision SMA 905 Connectors terminate the assembly and are precisely aligned to the spectrometer's slit to ensure concentricity of the fiber. Finally, captive end caps protect the fiber tips against scratches and contaminants.

(i) The software system:

Figure (3.7) shows the software "SpectraSuite" used in this work. It was supplied from Ocean Optics and it is a completely modular, Java-based

spectroscopy software platform that operates on Windows, Macintosh and Linux operating systems. The software controls the Ocean Optics USB spectrometer, as well as any other manufacturer's USB instrumentation using the appropriate drivers.

This software can easily manage multiple USB spectrometers – each with different acquisition parameters in multiple windows, and provides graphical and numeric representation of spectra from each spectrometer.

SpectraSuite allows you to perform the three basic spectroscopic experiments – absorbance, reflectance and emission – as well as signal-processing functions such as electrical dark-signal correction, stray light correction, boxcar pixel smoothing and signal averaging.

Using SpectraSuite, one can combine data from multiple sources for applications that include upwelling/down welling measurements, dual-beam referencing and process monitoring.

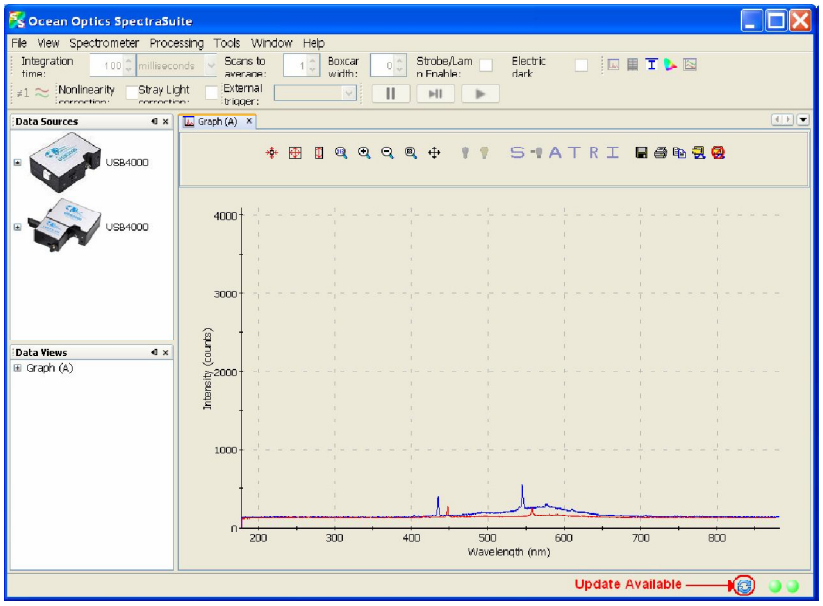

Figure (3.7): SpectraSuite software screen

3.5 Methodology:

1. The setup was arranged as shown in figure (3.1).
2. The laser energy was adjusted by adjusting the flash lamp voltage in order to obtained sufficient peak power needed to form plasma.
3. Then the spectrometer was connected to the PC through USB cable and the program spectra suit was launched.
4. The desired parameters (integration time, scans to average, and boxcar width) was set to ensure accurate data.
5. Then the optical fiber terminal aligned during laser operating till maximum intensity was collected and appeared on the screen.
6. A laser pulse was aligned on the cell with distilled water and the spectrometer recorded the spectrum and save as a dark spectrum.
7. Aqueous sample with known concentration were prepared by dissolving the chemical powders of heavy metals salts (oxides, chloride) and diluting it in distilled water for required concentration.
8. After that the sample was put in the cell and a pulse from the laser was operated and the plasma emitted spectrum was recorded.
9. A graph was plotted between concentration and observed intensity for each element of heavy metals (as a calibration curve).
10. The elements (atoms and ions) of the sample were identified with different intensities in the recorded by referring to the NIST atomic spectra database and references. This step was applied to all the five waste water samples.

11. Then the concentration of each heavy element was determined for each element from the calibration curve.

Chapter Four

Results and Discussion

Chapter Four

Results and Discussion

4.1. Introduction:

This chapter presents the data collected from the experimental work, in figures, and tables. The data was analyzed and discussed. The LIBS emission spectra were recorded at an angle of 90˚ to the direction of incident laser pulse. Software built in the spectrometer reads the data from the chip and reconstructs the spectrum. This makes it possible to measure a wide wavelength range simultaneously with high spectral resolution (0.03 nm).

The primary advantage of LIBS for liquid samples, such as the samples in this study, is that it can be used for direct qualitative and quantitative analysis of elements without any pretreatment and sample preparation. In this study, and for the optimization of various parameters of LIBS, the different stoichiometric samples of Mn, Cr, Mg, Ba, Fe, Cd, Hg, Co and Ti etc. were prepared in distilled water in order to be used as standard samples for concentration calibration.

4.2. The qualitative results:

4.2.1 Irradiation with 30 mJ :

Figures (4.1) to (4.5) show the LIBS emission spectra for the five waste water samples, respectively, after irradiation with 30 mJ pulse energy, the spectra were recorded in the region from 180 nm to 900 nm.

Atomic spectra database, and Hand book of Basic Atomic Spectroscopic Data were used for the spectral analysis of the samples, table (4.1) lists the analyzed data for the five samples.

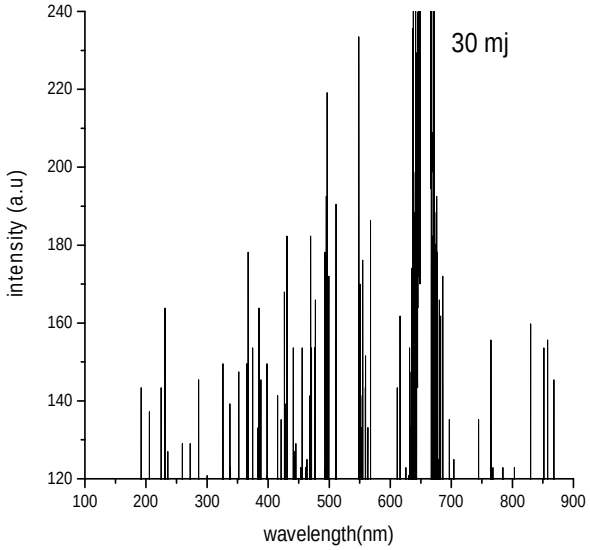

Fig (4.1): LIBS emission spectrum of sample (1)after irradiated by 30 mJ .

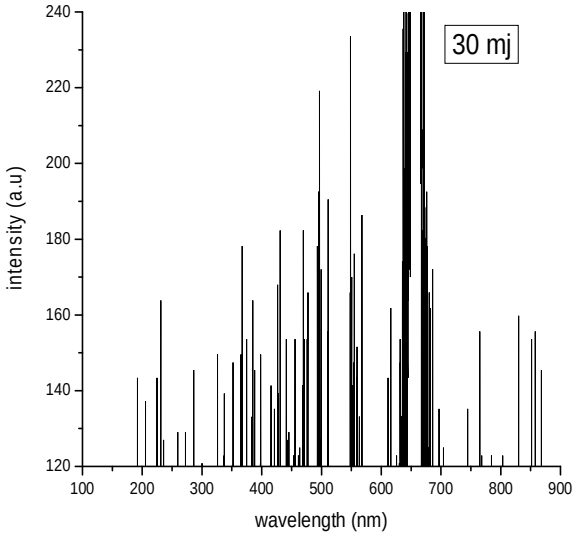

Fig (4.2): LIBS emission spectrum of sample (2) after irradiated by 30 mJ,

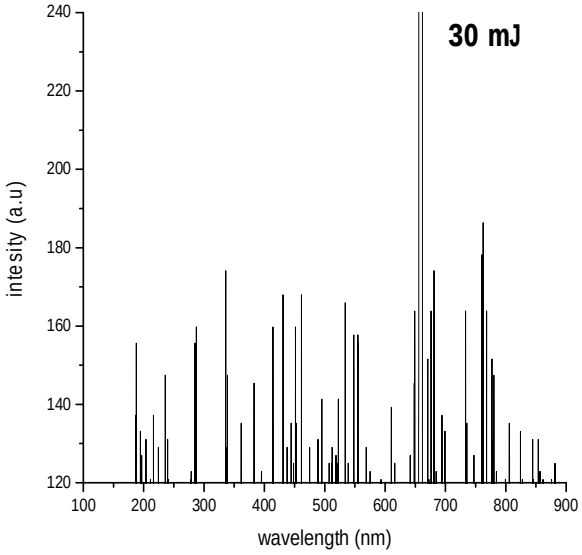

Fig (4.3): LIBS emission spectrum of sample (3) after irradiated by 30 mJ .

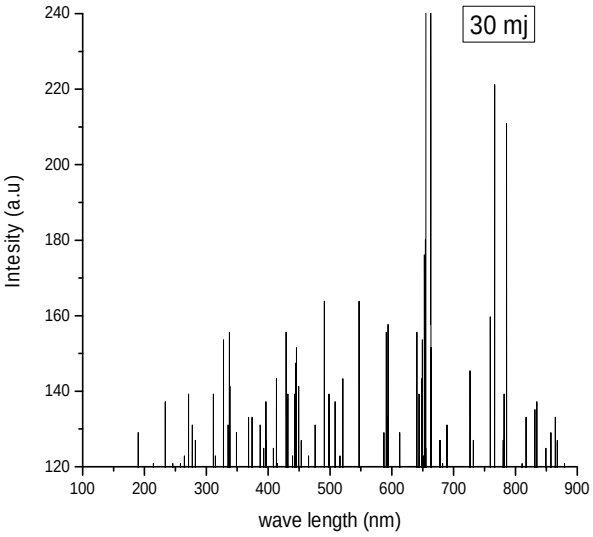

Fig (4.4): LIBS emission spectrum of sample (4) after irradiated by 30 mJ.

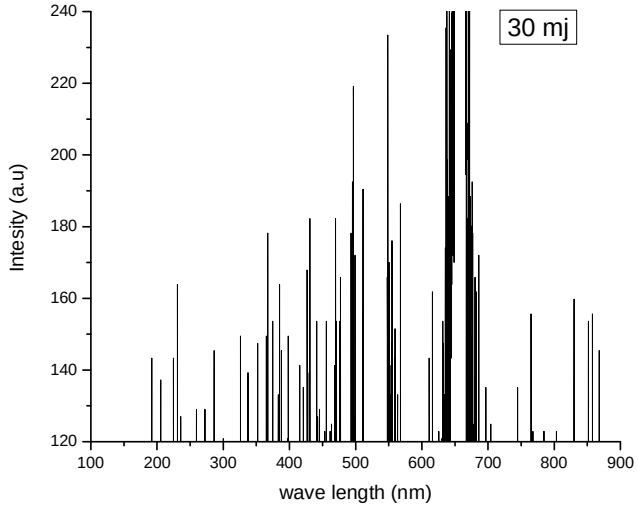

Fig (4.5): LIBS emission spectrum of sample (5) after irradiated by 30 mJ.

Table (4.1): The analyzed data of the five samples irradiated by 30mJ:

element	λ (nm)	I_{S1}(a.u)	I_{S2}(a.u)	I_{S3}(a.u)	I_{S4}(a.u)	I_{S5}(a.u)
Na II	420.87	140.75	140.97			
	476.85	129.12	171.44		131.27	
Na III	444.85	135.72	187.83		148.05	147.91
	535.16	166.64		167.73		
Fe I	249.62	115.33				
	278.60	123.26		123.38		
	326.29	108.9	155.06			
	344.24	115.46				
	373	115.13	153.56		133.30	
	334.58	174.17		175.92	139.33	
	415.21	159.97	141.51	161.67	143.36	143.65
	426.87	173.85	173.74	156.50	155.39	143.65
	452.86	128.62	128.51	160.14	127.40	
	456.86	159.10	158.99			
	513.17	129.61	190.99	130.70		
	517.17	127.29		129.06		
	550.84	158.17	220.54	157.95		155.71
	554.82	158.17	181.93	157.95		178.39
	743.06	140.8				
	768.72	165.49	128.51	164.12	223.15	157.81
	829.35	165.38				
Fe II	235.62	127.15	127.37	149.27		
	236.29	148.18	132.50			
	λ (nm)	I_{S1}(a.u)	I_{S2}(a.u)	I_{S3}(a.u)	I_{S4}(a.u)	I_{S5}(a.u)
	239.62	131.63	132.50	131.30		
	258.29	129.39	129.50			
	286.60	160.19	145.72	161.83	129.24	

	454.19	129.33	153.86		129.2	
	634.78					
	664.77		225.84			
	677.09	163.91	192.63	166.09		
Cr I	284.60	156.26		157.57		
	337.25	174.34	139.11	131.03	133.56	141.69
	374.90	154.18	158.99	158.47	135.66	155.91
	395.22	123.33	153.74	124.47	139.46	151.72
	675.76	201.64				
	769.73	164.12	123.00	165.93		
Cr II	272.27		134.47			131.14
	286.60	160.19	161.83			
Ti I	431.20	168.22	182.91	169.53	141.82	184.62
	470.86	181.78	182.75	129.39	131.92	155.71
	492.84	178.49	183.89	141.90	166.13	180.29
	609.12	139.82		141.19		
	681.19	174.56	166.14	175.92		
	693.09	137.69		138.89		
	363.23	135.40	149.81	139.93		
	281.27				128.97	
Cu II	508.82	125.40	196.13			
	655.09	220.49		222.12		
Co I	641.78	220.21	217.97		158.07	241.31
Co II	194.97	133.70	143.64	135.01		
	278.60	123.54		124.69		
	494.84	224.96	193.12			
	496.51	141.79		143.10		
	521.16			126.77		
	568.81	129.61	192.09			135.53
Hg I	800.71	138.41	128.51	121.29	112.4	113.7
	830.37	160.03	160.30	121.49	137.36	162.00
	844.33			132.88		
	851.35	159.15	154.17			
Cs II	204.64	137.64	137.20	132.94		139.39
	438.87	159.10	158.99			
	615.12			126.77		
Ba II	186.98			157.62		
Mn I	414.88	146.97	146.87	159.97	143.59	141.29
	446.20	129.33	219.67	135..72	155.91	131.33
Mn II	339.24	139.82	139.00	149.38		
	452.53	123.33		161.72		
Pr I	641.11	220.38		129.06		
	663.10			222.12	135.72	
	631.76	171.17				
Pr II	682.76		167.51			

4.2.2 Irradiation by 60 mJ:

The spectra of the five samples were recorded in the same region as shown in figures (4-6) to (4-10), the recorded spectra were analyzed and the identifications of each spectral lines are listed in table (4.2),

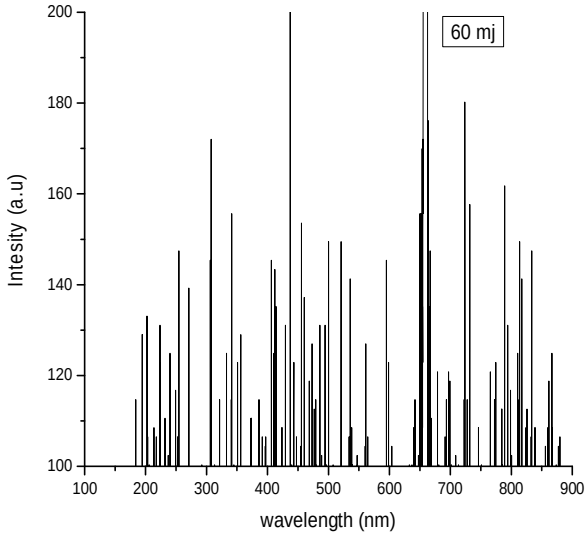

Fig (4.6): LIBS emission spectrum of sample (1) after irradiated by 60 mJ.

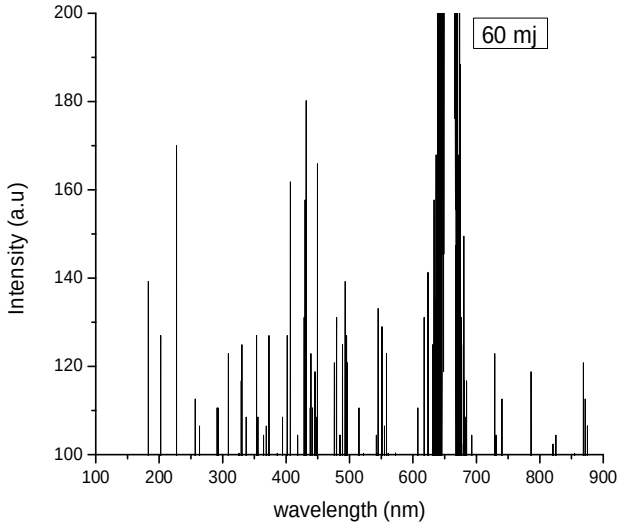

Fig (4.7): LIBS emission spectrum of sample (2) after irradiated by 60 mJ.

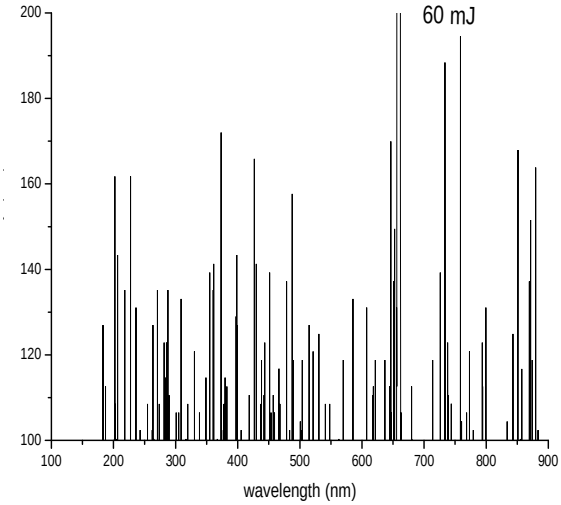

Fig (4.8): LIBS emission spectrum of sample (3) after irradiated by 60 mJ.

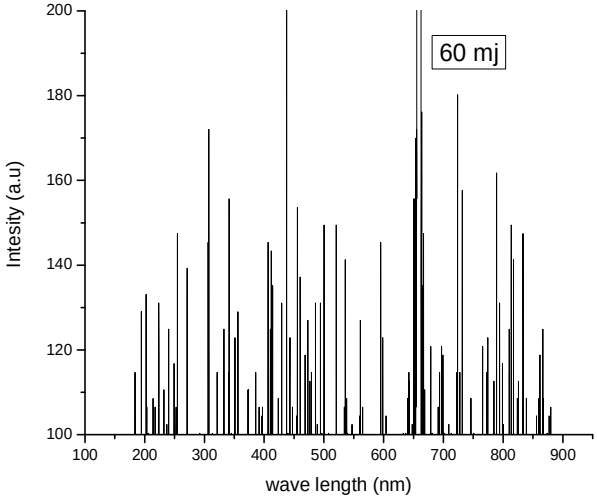

Fig (4.9): LIBS emission spectrum of sample (4.) after irradiated by 60 mJ

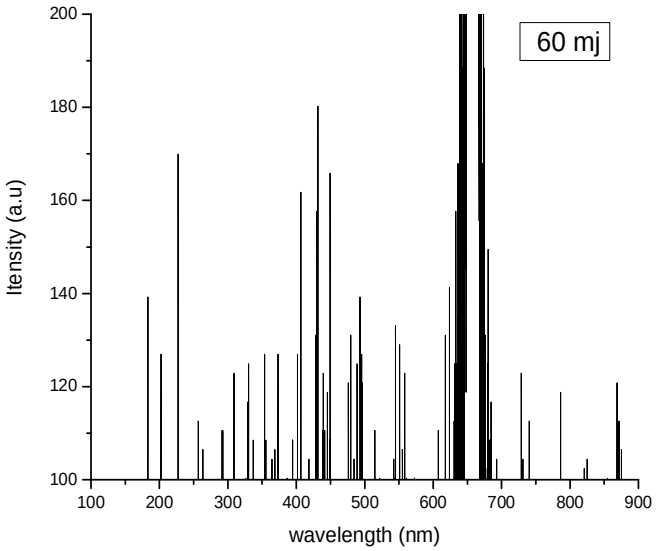

Fig (4.10): LIBS emission spectrum of sample (5) after irradiated by 60 mJ

Table (4.2): The analyzed data of the five samples, after irradiated by 60 mJ:

Element	λ nm	I(S_1) a.u	I(S_2) a.u	I(S_3) a.u	I(S_4) a.u	I(S_5) a.u
Na11	185.31	115	141.50	128.60	113.43	134.93
	329.25	126.55	126.16	119.98		125.16
Fe1	202.64	133.29	127.67	162.06	133.09	128.05
	305.79	145.87		107.01	163.65	122.47
	373.90	111.33	127.39	172.68	129.56	127.39
	415.86	145.67	162.42	102.68	146.87	162.71
	411.88	144.94	162.03		144.10	
	437.58	209.38	111.86	119.66	201.74	123.52
	484.40	130.67	104.72	102.75	132.62	104.98
	487.50	102.55	125.96	159.19	131.18	124.55
	666.77	148.17	163.12	107.34	136.24	220.98
	732.11	158.19		189.13	159.36	105.7
	793.71	132.62		123.20	131.85	
Fe11	182.98		140.26	127.78	115.33	141.75
	183.31			128.60		
	193.98	130.52	129.49		129.75	
	221.96	132.62		135.58	131,13	
	223.85	129.55			132.67	
	265.61		107.14	128.60		
	443.53	135.78	119.73	128.51	123.59	110.68
	451.53	160.41	165.63	124.32		
	454.19			107.27	155.34	

	501.84	150.97		104.52	149.67	
	551.15	158.44	130.48			131.46
	557.15		124.19	124.32		
	657.44	220.19		140.57	220.85	
	666.43					242.03
	757.44			201.66		
	813.71	150.97			150.13	
Cr1	438.53	209.05	123.73	119.72	209.77	125.17
	473.07	127.78	106.29	94.07	128.69	121.31
	617.12		132.58	113.43		
	720.79	179.62			181.91	
	833.67	149.14		105.24		
	227.96		170.22	167.37		172.43
	253.95	149.14		109.10		
	255.95	147.8	114.29	109	149.01	113.95
	356.39	130.14	127.54		130.48	
Cr II	559.81	128.69	123.21			
	727.42	115.27	123.34	140.57		
Ti1	271.61	140.24		136.64		
	351.91	123.33	128			129.17
	431.20	131.65	178.90	141.55	131.78	178.64
	470.92	127.46	124.78	120.12	127.46	120.64
	489.18	103.53	120.12	158.39	103.08	127.14
	640.78	107.20	201.39	115	115.33	221.96
Cu1	287.60		110.88	136.64		
	331.09	125.36		121.23	126.37	125.29
Co11	487.52	131.58	125.50	159.19	130.86	125.55
	240.47	125.82		103.2	126.37	
	271.81	139.97		135.71	140.62	
Cs11	373.23		128.65	109.10	111.33	127.98
	429.20		159.32	141.81	131.32	133.30
	595.80	146.78			146.40	
	652.44			150.26	171.33	
Mn11	329.92		125.77	121.16		127.21
	473.83	128.69	120.85			
	479.18	113.79	132.58	137.55	115.46	133.30
Ba11	536.13	142.73			142.93	
Mg1	765.99	120.90		112.38	121.95	118.87
	834.61	184.23		109.25	148.1	184.30

4.2.3 Irradiation by 80 mJ:

When pulse energy was irradiated to 80mj, some ions were appeared at higher order of ionization stages, like Cr IV, Ti III, Cs III, Mg III, figures from (4.6) to (4.10), table (4.3) illustrated that fact.

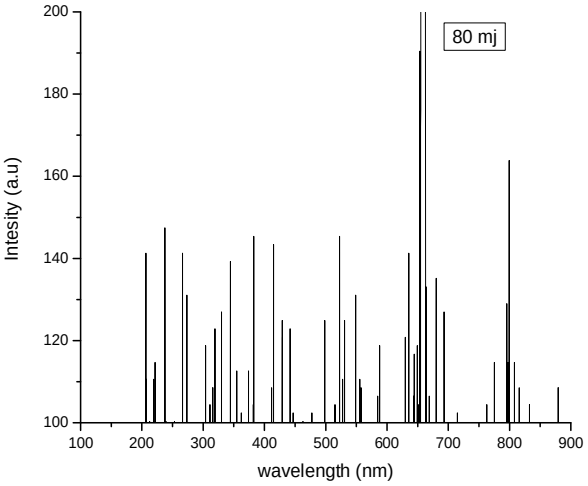

Fig (4.11): LIBS emission spectrum of sample (1) after irradiated by 80 mJ

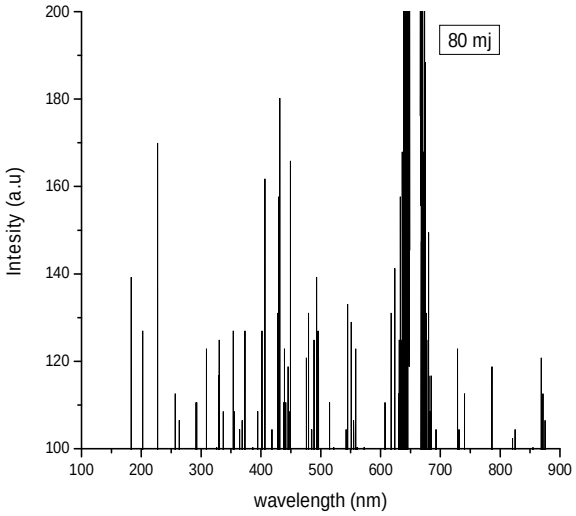

Fig (4.12): LIBS emission spectrum of sample (2) after irradiated by 80 mJ

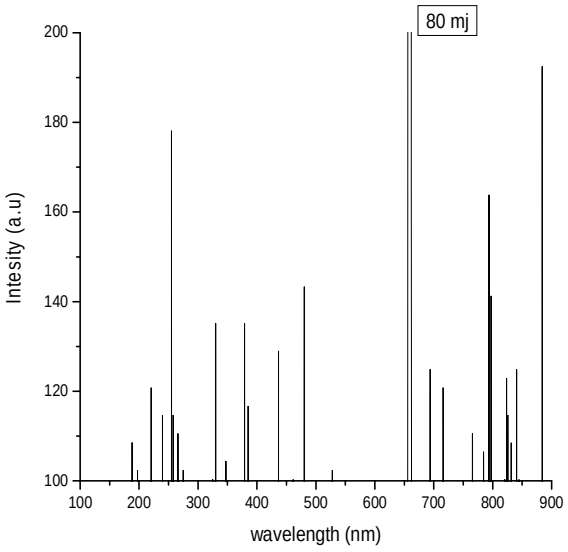

Fig (4.13): LIBS emission spectrum of sample (3) after irradiated by 80mJ.

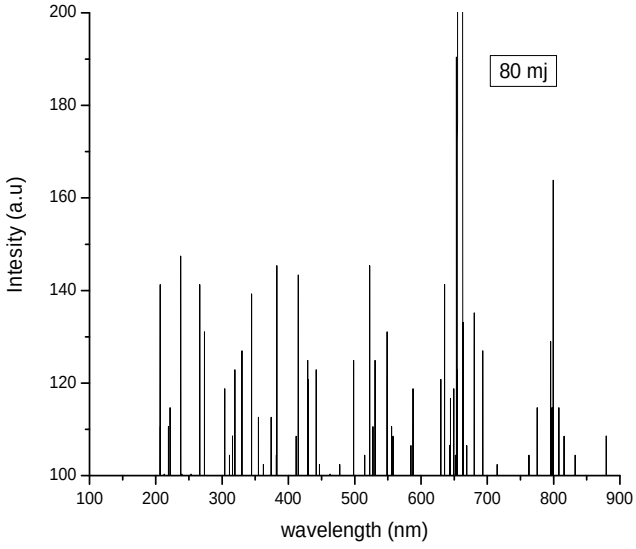

Fig (4.14): LIBS emission spectrum of sample (4) after irradiated by 80 mJ.

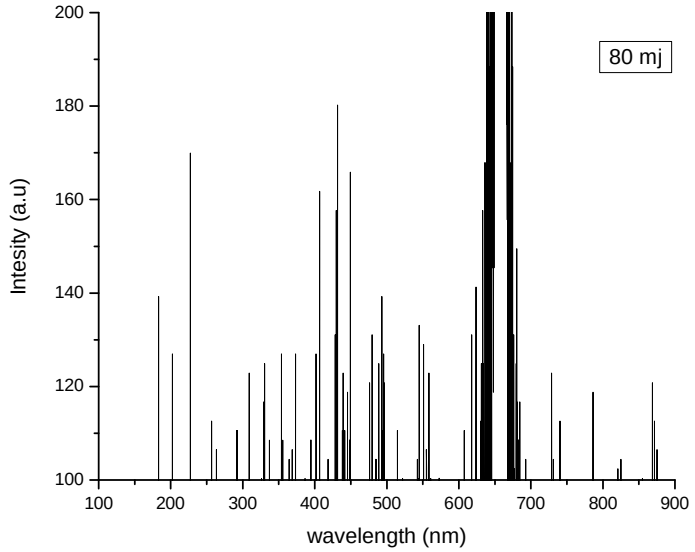

Fig (4.15): LIBS emission spectrum of sample (5) after irradiated by 80 mJ.

Table (4.3): The analyzed data of the five samples after irradiated by 80mJ:

Element	λ (nm)	I(S_1) a.u	I(S_2) a.u	I(S_3) a.u	I(S_4) a.u	I(S_5) a.u
Cs I	328.92			136.15	129.10	
Cs II	429.20				127.73	158.13
Cs III	206.30				143.46	
Fe I	227.43					173.09
	271.9	130.96	129.61			
	344.6	139.70				
	371.87	112.99				
	374.14	115.34	127.76		135.66	127.06
	415.21	144.29	142.06	160.03	145.95	104.71
	498.38	125.34	172.26		141.82	221.45
	514.24	104.6	190.50			
	545.56		133.49			
	550.84	131.40	129.74			
Fe II	220.84	114.96				
	262.26		107.34			
	529.34	125.55				
	221.90	111.19		121.14		
	233.29				139.59	166.13

	832.18	104.91		108.63	127.47	
Cr I	238.29	148.17				
	267.71	141.78				
	387.89	164.01	164.34		131.46	147.78
	407.80		162.24			163.30
	435.32		129.16			
	493.63		139.76			140.24
	514.23	104.69	111.23			110.28
Cr II	205.33	141.61			149.75	
	274.27				133.63	
	258.21					115.06
	618.23		131.27			
Ti I	237.96	147.67				129.56
	268.04	141.29				
	322.97	122.88				
	331.10	118.18		135.39		125.16
	337.83		109.25			109.24
	352.94	112.83				126.87
	428.90	125.23	139.66	168.33	158.33	184.62
	529.72	125.23				
	548.82	130.96	220.76	153.15	133.56	233.83
	799.37	164.33			166.26	
Ti III	608.06		111.01			
	498.84				127.40	
CuI	693.58	126.54	105.43			
	302.78	119.01				
Cu11	662.43				242.62	
CoI	240.72					
	339.53			109.36		
	344.91					
	345.35	139.59		104.44	141.56	
	357.53	139.59		94.81		
CoII	228.68		170.57			
	727.48		123.32			

HgI	302.14				118.87	
	404.65	94.68				
	579.06	90.02				
	681.16	135.28				
	833.69	104.96		108.33		
Hg11	203.17					142.35
	205.28	103.13			143.64	
	794.45			162.97		129.97
Mn1	259.72			114.80		131.14
Mn11	353.38	127.83				
	431.12		180.74			180.54
	883.15			191.75		
	654.44				242.62	
	182.65					142.35
MgI	775.92	114.96				
Mg III	293.67		111.01			
	480.26		143.75			
MoI	309.22		123.24			
	384.72			116.60		
	523.83				147.98	
	785.44			106.55		

4.2.4 Irradiation by 100 mJ:

When pulse energy was irradiated to 100mJ, some ions were appeared at higher order of ionization stages, like CrIV, Ti III, Cs III, Mg III figures from (4.16) to (4.20), table (4.3) illustrated that fact.

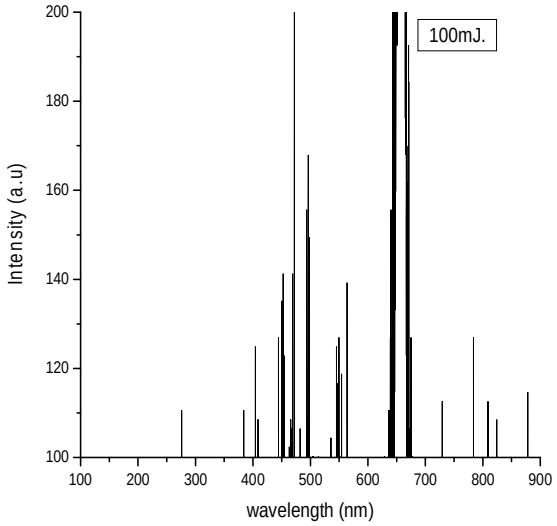

Fig (4.16): LIBS emission spectrum of sample (1) after irradiated by 100 mJ.

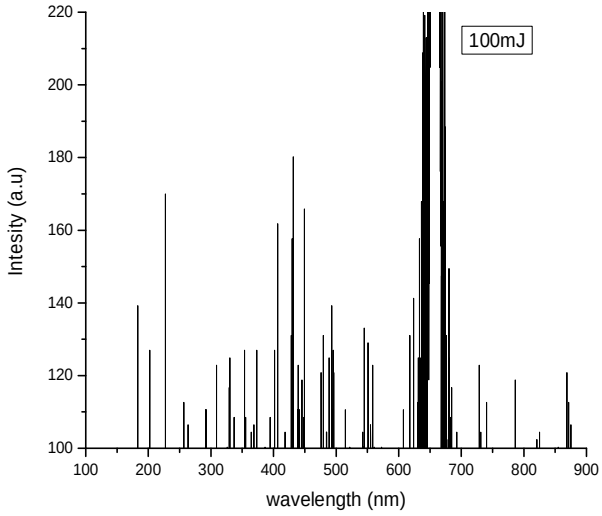

Fig (4.17): LIBS emission spectrum of sample (2) after irradiated by 100 mJ.

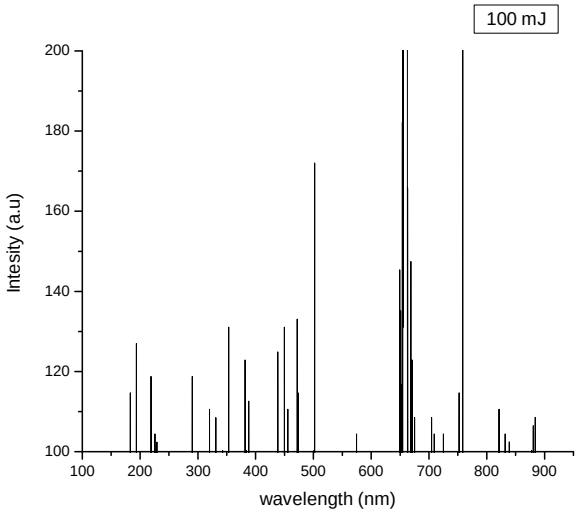

Fig (4.18): LIBS emission spectrum of sample (3) after irradiated by 100 mJ...

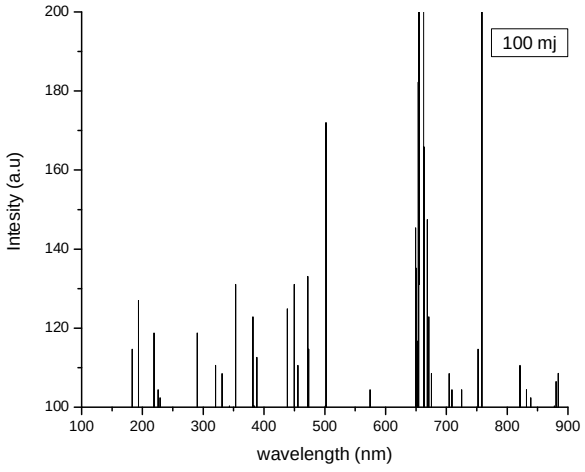

Fig (4.19): LIBS emission spectrum of sample (4) after irradiated by 100 mJ

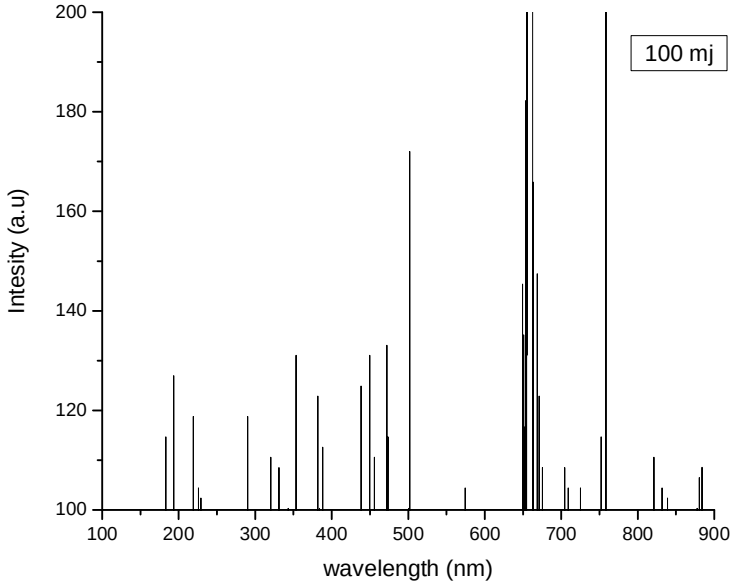

Fig (4.20): LIBS emission spectrum of sample (5)after irradiated by 100 mJ

Table (4.4): The analyzed data of the five samples after irradiated by 100 mJ.

Element	λ (nm)	I(S_1) a.u	I(S_2) a.u	I(S_3) a.u	I(S_4) a.u	I(S_5) a.u
Cs11	652.44				184.43	
Cs111	676.16					129.22
	206.30				143.46	
Fe 1						
	289.94	118.90				
	545.56		125.46			
	550.84		127.07			
	228.76				105.13	
	228.76				105.13	
	449.46					138.30
	550.84					129.66
Fe11	183.07				116.87	
	274.27				133.63	
	668.68				149.53	
	757.04				202.23	
	855.70					
	880.89				108.46	
	752.50			106.77		
	808.02					115.06

	752.50			106.77		
	472.80		203.21			
	808.02		113.07			
	192.14	127.14				
	226.88	104.48				
	750.65	114.80				
	757.04	200.30				
	832.60	104.48				
Fe111	408.10				111.08	
Cr1	823.56					111.23
	832.18				106.11	
	823.57		108.72			
Cr11	451.17				133.31	
	238.29				149.75	
	321.65				112.45	
Cr IV	242.33			110.81		
Ti1	289.93				120.69	
	729.96		112.39			
	331.10	108.63				
	573.90				106.11	
Ti 11	694.53			108.57		
	694.53			108.57		
Cu11	353.37				133.09	
	444.49	129.74				
Co11	496.43		168.36			
	275.32					113.15
	330.75				110.48	
	496.43		168.36			
Hg1	470.30			143.81		
Cs11	652.44				184.43	
	470.30					143.81
Cs111	676.16					129.22
Mn11	353.38	131.35				
	472.78					207.73
	667.76					241.60
	676.16					129.22

Pr11	410.07			139.43		
Mg111	192.13				128.89	
	472.32				135.00	
Ba1	408.73		108.87			

4.3 The Quantitative results:

To calculate the concentrations of the metals that were appeared in the samples, calibration curves were plotted for different metals, using known concentrations and irradiated by pulse energies of 30, 60 mj.

4.3.1 The Calibration Curves for Metals:

Different stoichiometric metals mainly: Mn, Cr, Ba, Mg, Ti, Fe, Hg, and Co in liquid phase were prepared. For this purpose pure metals in powder salts form were mixed in distilled water with various known concentrations: 500 ppm, 1000 ppm, 2000 ppm, to 12000 ppm. LIBS spectra were recorded for these known concentrations of each element. From the calibration curves the concentrations of the deferent heavy metals in the dairy samples were calculated.

Figures (4.21) to (4.26), illustrated the calibration curve of the elements obtained by drawing the elements emission intensities ($Intensity_1$) against the concentrations in the metals salts (N_1).

From these calibration curves N_1 was determined for each metal, and it was used in equ. (4.4) to calculate the concentration (N_2) of each metal which was presented in the sample.

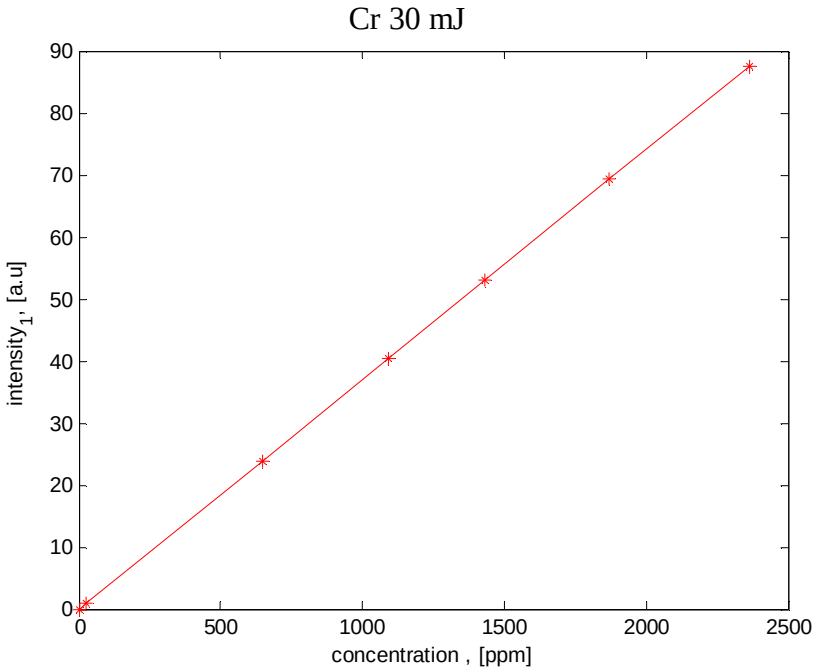

Fig (4.21): calibration curve of Chromium after irradiated by 30 mJ.

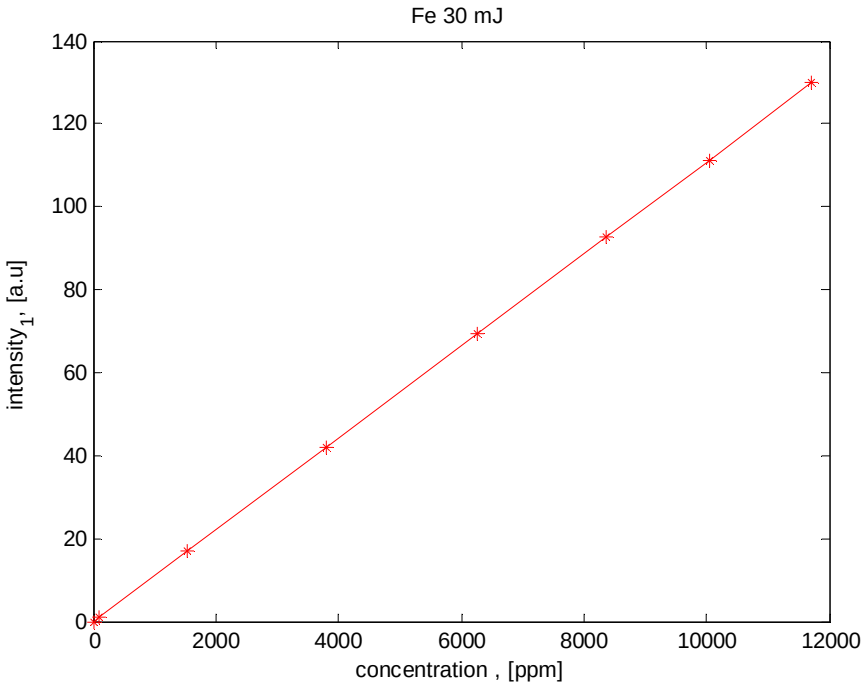

Fig (4.22): calibration curve of Iron after irradiated by 30 mJ.

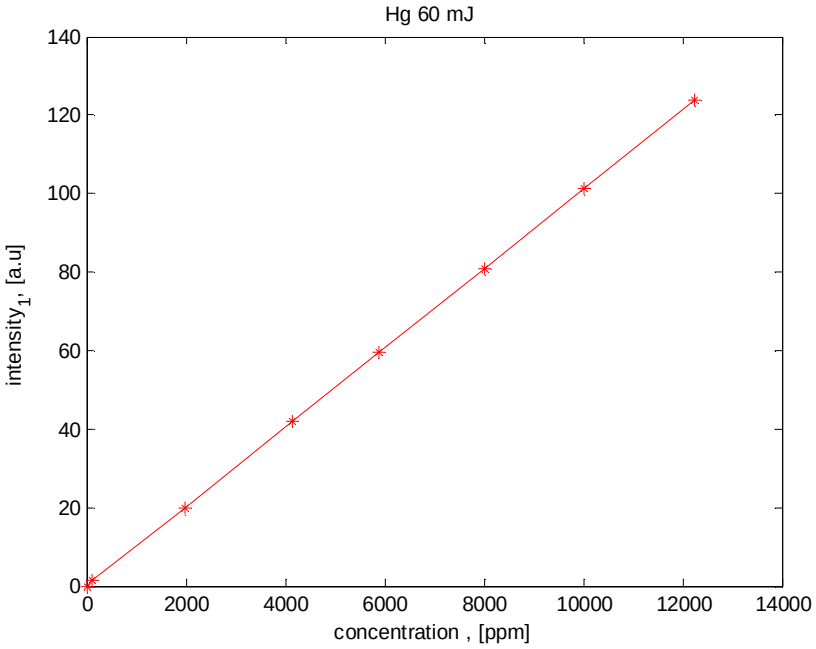

Fig (4.23): calibration curve of Mercury after irradiated by 60 mJ.

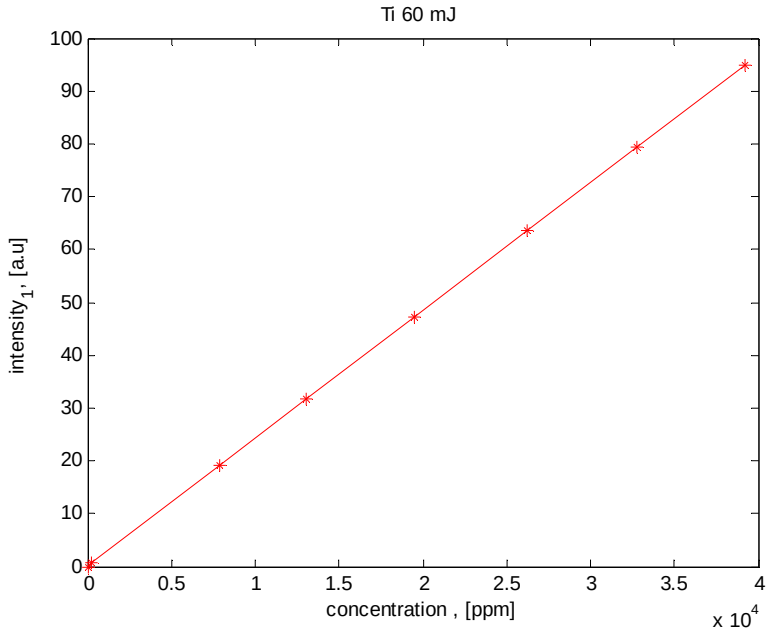

Fig (4.24): calibration curve of Titanium after irradiated by 60 mJ.

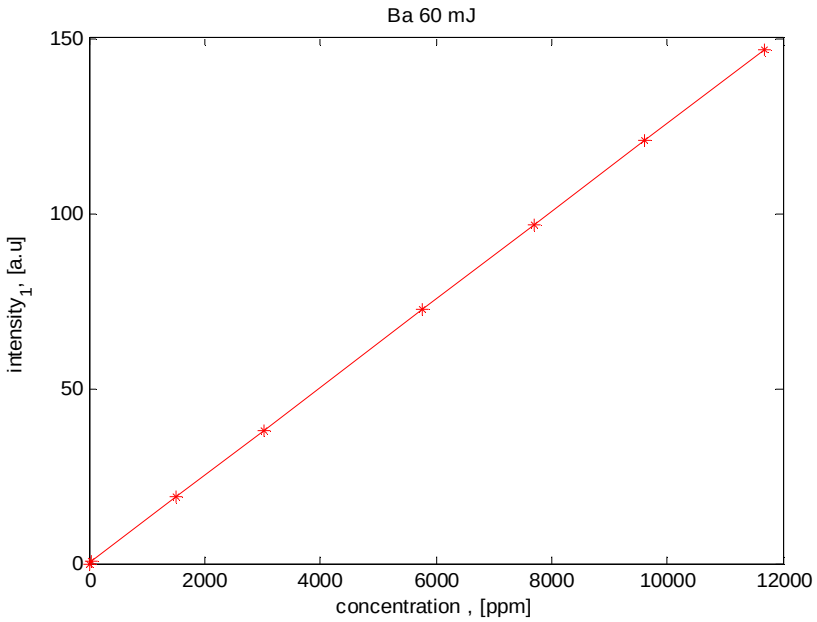

Fig (4.25): calibration curve of Barium after irradiated by 60 mJ.

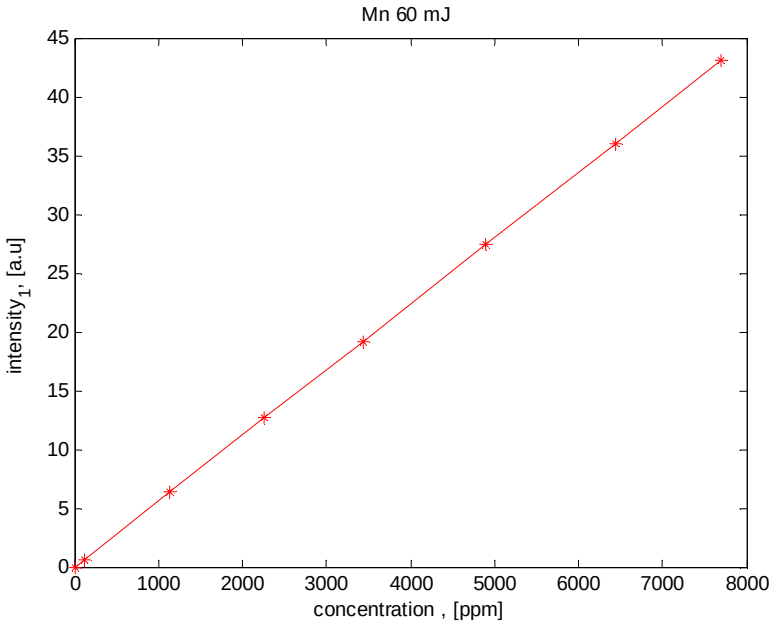

Fig (4.26): calibration curve of Mangenies after irradiated by 60 mJ.

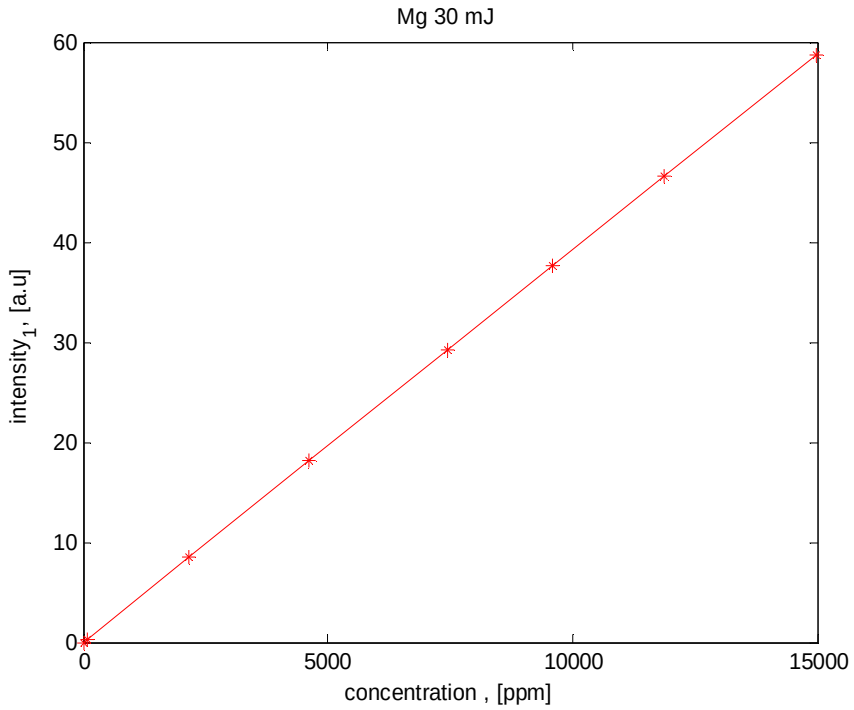

Fig (4.27): calibration curve of Magnisium after irradiated by 30 mJ.

4.3.2 Calculation of concentration:

The number of atoms for each metal per unit volume was calculated from equation (4.1):

$$I = \frac{hcANg}{4\pi\lambda U} e^{\left(-\frac{E}{KT}\right)} \qquad (4.1)$$

Where A is the spontaneous emission coefficient of the given transition, h is the Planck constant and U is an instrumental factor depending on the experimental set-up used. This relation is valid only when the considered u_l transition is optically thin, that is, not suffering from self-absorption, a condition that can severely affect low-energy and resonance lines, particularly for high-concentration elements. Several methods can be found in the literature to evaluate and correct the self-absorption, and a good practice in analytical LIBS is to select accurately the

emission lines to be used for analysis. Table (4.5) and (4.6) show The calculated concentrations of different metals presented in samples.

The number of atoms per unit volume of observed metals can be determined from the ratio of the intensities of neutral to neutral lines. And if the plasma is in local thermal equilibrium then the observed intensity of an excited state, I is proportional to the density of neutral atoms or ions of this element. The intensity ratio of two lines belonging to the same atomic species is given by :

$$I_1 = \frac{hcA_1 g_1 N_1}{4\pi\lambda_1 U1} e^{(-E_{1/KT})} \qquad (4.2)$$

$$I_2 = \frac{hcA_2 g_2 N_2}{4\pi\lambda_2 U_2} e^{(-E_{2/KT})} \qquad (4.3)$$

Where I_1 is the intensity of the first spectral line, and Where I_2 is the intensity of the second spectral line.

The concentration is given by:

$$\frac{N_2}{N_1} = \frac{A_1 g_1 \lambda_2 I_2}{A_2 g_2 \lambda_1 I_1} \frac{exp(-E/KT)}{exp(-E/KT)} \qquad (4.4)$$

Then

$$N_2 = \frac{A_1 g_1 \lambda_2 I_2 N_1}{A_2 g_2 \lambda_1 I_1} \frac{exp(-E_1/KT)}{exp(-E_2/KT)} \qquad (4.5)$$

By taking the natural logarithm of both sides of equ.(4.5).Then N_2 calculated for each metal by using matlab program, as shown in table (4.5), and (4.6).

From the two tables (4.1), and (4.2), N(s) is the concentrations of the metals in the samples at pulse energies 30, 60 mJ in ppm, and (λ) is the wavelength of the metals appeared in graphs (4.1) to (4.10), and tables (4.1) and (4.2). These wave

lengths were used in equ. (4.5) also it was obtained from these tables, and I is the transmitted intensity also obtained from tables (4.1), and (4.2).

Table (4.5): The calculated concentrations of different metals presented in samples. irradiated by 30 mJ.

Metals	λ (nm)	$N(s_1)$ (ppm)	$N(s_2)$ (ppm)	$N(s_3)$ (ppm)	$N(s_4)$ (ppm)	$N(s_5)$ (ppm)
Cr	473.07	52	23	21	58	56
Fe	415.86	37	38	32	36	40
Hg	800.71	42	94	69	74	79
Mn	446.20	31	39	31	33	23
Ti	431.20	47	20	159	29	27

Table (4.6): The calculated concentrations of different metals presented in samples. irradiated by 60 mJ.

Element	λ (nm)	$N(s_1)$ (ppm)	$N(s_2)$ (ppm)	$N(s_3)$ (ppm)	$N(s_4)$ (ppm)	$N(s_5)$ (ppm)
Cr	438.53	17	27	13	18	21
Fe	415.86	28	37	13	18	19
Mg	765.99	87	96	-	400	180
Ti	431.20	22	20	133	26	25

4.3.3 Limit of detection (LOD):

In order to enhance the sensitivity of the LIBS system, for analysis of waste water samples, the optimal experimental conditions, which can affect the limit of detection (LOD) in LIBS, were investigated. Prior to the analysis of dairy product

waste samples, different parameters such as laser energy and the focal length of the focusing lens, were optimized

$$LOD = 2\sigma / s \qquad (4.7)$$

Where in above equation σ is the standard deviation of background noise level and s is calibration sensitivity (slope of the calibration curve). Table (4- 7) lists the value of these parametry, obtained from figures (4.21) to (4.26).

Table (4.7): The slope, standard deviation and limit of detection.

Element	Standard deviation	Slope	LOD
Fe I	0.26	0.068	34
Cr I	0.65	0.019	68
Ti I	0.33	0.002	30
Mn I	0.16	0.005	165
Mg I	0.22	0.001	220
Co I	0.31	0.040	7
Ba I	0.26	0.019	13
Hg I	0.39	0.010	39

4.4 Discussion:

The five samples was irradiated by pulse laser energy 30 mJ, and the spectra of these samples were recorded as shown in figures (4-1) to (4-5), the recorded spectra were analyzed and the identifications of each spectral lines are listed in table (4.1). This table illustrate that the atoms was excited to the excited states.

The five spectra of the samples showed different amounts of elements, include heavy elements like (Na, Co, Cu, Fe, Cs, Hg, Pr, Cr, Ti, Mn, Mg,), that were found in all samples with different irradiated pulse energy.

It is clear from table (4.1), that the sodium ions were appeared in samples (1,2,4) and disappeared in samples (3, and 4), due to location of the sample. Sodium ions was appeared in higher order of ionization because the laser energy can excited the energy states, the irradiated pulse energy was sufficient to excited this metal.

Iron atoms were appeared in all five samples with higher amount especially in sample (2 and 4), also Iron ion was appeared with high amount in all samples at pulsed energy 30 mJ.

Chromium atoms were found at different amount, the energy states of it can excite with low pulse energy. In sample (1) these atoms were presented with high amount, while Cr is toxic metal even it found with little amount.

Mercury atoms (Hg) was found with relatively little amount in the all five samples, (this element is highly toxic even with little amount).

Beside neutral atoms, ions of different amounts and ionization stages also were recorded as shown in Table (1). All these ions may not present in the sample originally, where some of them are produced due to the ionization of neutral atoms by the laser power density.

The pulse energy was increased to 60 mJ and the spectra of the five samples were recorded in the same region as shown in figures (4-6) to (4-10), the recorded spectra were analyzed and the identifications of each spectral lines are listed in table (4.2), the emission intensity of the metals were increased .

This table illustrate that the number of atoms in the excited state was increased, this due to increasing the pulse energy.

The increasing of pulse energy to 60 mJ was increase the amount of chromium atoms. Cesium ion (Cs^{+1}) was presented with relatively little amount in samples (2, 3, 4, and 5), and disappeared in samples (1). Also Cobalt ion (Co^{+1}) was found with low amount in samples (1, 3, 4), while in samples (4, and 5) it was not found due

to component of the samples. The copper ion (Cu^{+1}) was found with relatively high amount in samples (1) and (2) at 30 mJ.

The Iron ion (Fe^{+1}) was found in sample (2) with very high amount compared with the other three samples (1, 3, 4) at 30mJ, and was not found in sample (5), this due to location of the sample which was collected from, and the power density of the laser densit . When the samples was irradiated by 60 mJ, Fe^{+1} was presented with high amount in sample (2) also.

The sodium ion (Na^{+1}) was found in relatively high amount in sample (2), and little amount in samples (1, and 4), and was not presented in samples (3, and 5) due to the component of the sample.

Beside neutral atoms, ions of different amounts and ionization stages also were recorded as shown in Table (4.1) to (4.5). All these ions may not present in the sample originally, where some of them are produced due to the ionization of neutral atoms by the laser power density.

The pulse energy was increased to 80 mJ and the spectra of the five samples were recorded in the same region as shown in figures (4-11) to (4-15), the recorded spectra were analyzed and the identifications of each spectral lines are listed in table (4.4). sample (1) had large amount of metals, most of ions was appeared at different ionization stages by the laser power density.

Fe, Fe^{+1}, and Ti, atoms were appeared with relatively high amount in all five samples. Cr, and Cr^{+1} were found with high amount due to the pulse energy,

CsI, Cs II, and CsIII were presented in sample (4), also Cs II was appeared in ample (5). The number of ion in Cu^{+1} was increase, and appeared with highly amount in sample due to increasing the pulse energy to 80 mJ.

Ti III was found in samples (1, and 2), and Co atoms was appeared in samples (1, 3, and 4) with little amount. Co^{+1} was appeared in samples (2, 3, and 4) with higher amount than Co atoms.

Mn II was presented in all five samples with high amount due to sufficient pulsed energy, Hg II was appeared in four samples and disappeared in sample (2).

Hg atoms was presented with little amount in sample (1) and relatively high amount in samples (3, 4, and 5). Mn atoms was found with little amount in samples (3, and 5).

The pulse energy was increased to 100 mJ and the spectra of the five samples. were recorded in the same region as shown in figures (4-16) to (4-20), the recorded spectra were analyzed and the identifications of each spectral lines are listed in table (4.4), sample (4) had high amount of metals.

Fe^{+1}, and Fe^{+2}, were founded in sample (4), that mean these metals this pulsed energy was sufficient to ionized most of Fe atoms. Also Fe^{+1} was presented in sample (5). In sample (2), Ba, and Cr atoms was found with little amount,

Increasing of the pulsed energy to 80 mJ, and 100mJ appearance ions or atoms in some elements with low amount, like appearance of CsIII, CrIV, MgIII, and Ti III at 100mJ. Hg atoms was appeared with little amount in samples (3), also Chromium ion (Cr^{+1}) presented with little amount in sample (2, and 4). Also

Cu II was presented relatively high amount in samples (1, and 4).

It is clear that from these results: the amount of different atoms and ions of metals appeared in all five samples depend on the power density of the laser, and the source of samples which was collected from. And also the ionization of neutral atoms depend on the laser power density.

Figures (4.21) to (4.26) show the plot of dependence of the intensity at laser pulse energy 30, and 60 mJ, via concentration. Concentration here is the number of atoms per unit volume.

Concentration was decreased by increasing the pulse energy some of atoms was appeared as ions at different ionization stages, this lead to decreasing the emitted intensity of them.

Cr, and Fe in sample (3) had lowest concentrations in all five samples, at irradiated pulse energy 30mJ , also Cr and Fe had low concentration in sample (3), at irradiated pulse energy 60mJ. Mn, and Ti were founded at low concentration in samples (2), and (5) respectively, due to the component of the sample, and irradiated pulse energy. Hg was appeared at high concentrations in all five samples, the highest in sample (2), due to location of the sample collection.

Ti appeared with low concentration in sample (2), while it had the highest concentration in sample (3), at 30, and 60 mJ, but was decreased when the pulse energy was increased to 60 mJ.

The calculated concentration of Mg at 60 mJ, was low in sample (1), and it was very high in sample (4). This concentration was the highest in all samples at different pulse energy.

From all these results, the concentrations of all samples were decreased by increasing of pulse energy of the laser and decreasing of emitted intensity as shown in tables(4.6), (4.7).

4. 5. Conclusions:

From the obtained results one can conclude that:

1. The analysis of the industrial water samples using LIBS technique led to the determination of different heavy metals.
2. The concentrations of heavy metals (Cr, Co, Fe, Mg, Ti, Mn, and Hg, present in waste water samples, were estimated and results achieved are in good agreement.
3. Cr and Hg atoms were appeared in all samples with different concentrations at different pulse energies, these atoms are highly toxic.
4. This study reveals that the waste water samples collected from diary plant are contaminated by several toxic elements Titanium, chromium, and Mercury. Most of these elements are considered as highly toxic and

carcinogens. They could cause a lot of problems for heart and lungs deceases.

4. 6. Recommendations:

The followings can be suggested as future work:

1. There is a need to establish a correlation between the used power density and the ionization energy of each heavy element.
2. Double pulse lasers can be used to enhance the detected signal.
3. The LIBS system can be used as a portable system for on line analysis of waste water from dairy products manufacturing plants. Investigations should be made to reduce the size and the initial cost of the instrumentation.
4. It is better to use evacuation system to get more accurate results.
5. It is better to use delay time system to control and uniform the measurements instead of manually capturing the spectra.

References:

- A. R. Striganov and N. S. Sventitskii, (1968) "Tables of Spectral Lines of Neutral and Ionized Atoms", New York: IFI/Plenum.
- Anna P. M. Michel, Marion Lawrence-Snyder, S. Michael Angel, et al., (2007): "Laser-induced breakdown spectroscopy as a promising in situ technique for oceanography", Optical Society of America. Vol. 46, No. 13 _ Applied Optics, (2507, 2509,20514).
- A. R. Striganov and N. S. Sventitskii, (1986) "Tables of Spectral Lines of Neutral and Ionized Atoms" IFI/Plenum, New York,
- Asli Baysal, Nil Ozbek and Suleyman Akman (2013) "Determination of Trace Metals in Waste Water and Their Removal Processes", chapte 7. open access article http://dx.doi.org/10.5772/52025, 146\ 148\ 156.
- Baysal et al. (2013): licensee In Tech. open access article distributed under the terms of the Creative Commons Attribution License (http://creativecommons.org/licenses/by/3.0).
- Boudjemai, S, Gasim, et. al., (2004): "Temporal characteristics of laser spark emission spectra".
- David A. Cremers and Leon J. Radziemskil, (2006): " Hand book of Laser-Induced Breakdown Spectroscopy", John Wiley & Sons Ltd, England.
- Fang.Yu Yueh, Jagdish P. Singh, and Hansheng Zhang, (2010): "Laser-induced Breakdown Spectroscopy Elemental Analysis", USA.
- Fitzpatrick, (1998): "Introduction to Plasma Physics" Austin.
- Franz Mayinger, (1994): "Optical Measurements", springer (Verlag) Germany.
- Halina Abramczyk, (2005): "introduction to laser spectroscopy", Elsevier, Poland.

- Hestekin, J.; Sikdar, S.; Bhattachayya, D.; Bachas, L.; et al., (2000): "Advanced Aspects of Spectroscopy", springer, USA.
- http://creativecommons.org/licenses.
- Jagdish P. Singh, Surya N. T hakur (2007), "Laser-Induced Breakdown Spectroscopy", Elsevier, uk
- J. E. Sansonettia , and W. C. Martin, (2005), " Handbook of Basic Atomic Spectroscopic Data", American Institute of Physics, Phys. Chem. Ref. Data, Vol. 34, No. 4.
- J. E. Sansonettia… and W. C. Martin, (2005), "Hand book of Basic Atomic spectroscopic data", American institute of physics, DOI: 10.1063/1.1800011.
- J. Michael Hollas, (2004): "Modern Spectroscopy", John Wiley & Sons Ltd, England.
- J., "Demtröder, (2008): "Laser Spectroscopy Vol.2,: Experimental Techniques", 4th ed., Springer, Germany.
- Jerry Workman, (1997): "Optical Spectrometers", North Sutton, New Hampshire.
- Karl F. Renk, (2012): "Basics of Laser Physics", Springer, Germany.
- Kim and Lin, licensee InTech. open access chapter distributed (http://creativecommons.org/licenses/by/3.0).
- Kim T, Nguyen B, Minassian V, Lin C.T, (2007): "Paints and coatings monitored by laser-induced breakdown spectroscopy". Optical Society of America, USA, Vol. 46, No. 13, Applied Optics.
- Kim T, Specht Z, Vary P, Lin C. T. (2004): "Spectral fingerprin of bacterial strains by laser induced breakdown spectroscopy" Optical Society of America, USA, Vol. 51, No. 7.

- L. J. Radziemski, Spectrochim. Acta, (2002): "from laser to LIBS the path of technology development.
- Latresa J. Williamson (2010): "Trace Elemental Analysis of Selenium and Antimony Using Hydride Generation Coupled to Laser Induced Breakdown Spectroscopy", PhD theises, .
- Leon J. Radziemski, Richard W. Solarz, and Jeffrey A.Paisner, (1987): "Laser Spectroscopy and Its Applications", Marcel Dekker, Inc. New York.
- Matthew Weidman1, Matthieu Baudelet, Santiago Palanco, et al., (2009): "Double pulse irradiation with Nd:YAG and CO_2 lasers as Laser-induced breakdown spectroscopy (LIBS) ". Optical Society of America, USA.
- Monica Simileanu, Roxana Radvan, Niculae Puscas, (2010): "LIBS setup for identification of metals underwater", U.P.B. Sci. Bull., Series A, Vol. 72, ISSN 1223-7027 Iss. 4.
- Peichao Zheng, et al., (2014): " Trace mercury in an aqueous solution using laser-induced breakdown spectroscopy with the assistance of a solution cathode glow discharge (SCGD) system". Springer-Verlag.
- Prefetti, B. M. (1994): "Metal Surface Characteristics Affecting Organic Coatings", Federation Series on Coating Technology, FSCT, Blue Bell, PA. Prof. Dr. Alexander Piel, (2010): "plasma physics", Springer, Germany (Berlin).
- Qassem I, et. al., (2012): "Bacterial identification by LIBS to identify pathogens in a clinical specimen", Applied Optics / Vol. 51, No. 7.
- Qi Shi, et.al. (2014): "Exploration of a 3D nano-channel porous membrane material combined with laser-induced breakdown spectrometry for fast and sensitive heavy metal detection of solution samples", **J**. Anal. At. Spectrom., 29, 2302-2308 DOI: 10.1039/C4JA00220B .

- R. Payling and P. Larkins, (2000) "Optical Emission Lines of the Elements", Chichester: John Wiley.
- Rai *et al.*,2001; Uhl *et al.*, 2001; Russell *et al.*, (2005): Richard Fitzpatrick, (1998) "Introduction to Plasma Physics", Springer, Austin.
- Roman Domański, Maciej Jaworski, Marek Rebow, (1995): "Laser Radiation Interaction with Solids".
- Rosalba Gaudiuso 1, Marcella Dell'Aglio 2, Olga De Pascale 2, Giorgio S. Senesi 2, et al., (2010): " LIBS applications to qualitative and quantitative elemental analysis in the broad fields of environmental science", Bari, Italy.
- Schmidt, N.; Goode, S. (2002), "Appllied Spectroscopy", Neenah, Wisconsin.
- Stamenkovic, J., Cakic, S., Konstantinovic, S., Stoilkovic, S. (2004): "Catalysis of the Isocyanate- Hydroxyl Reaction by Non-Tin Catalysts in Water borne Two Components Polyurethane Coatings", Bari,Italy
- T. Hussain Æ M. A. Gondal, (2008): "Detection of Toxic Metals in Waste Water from Dairy Products Plant Using Laser Induced Breakdown Spectroscopy", springer, Pakistan, 561\ 562\563.
- T. Hussain AE. M. A. Gondal, (2007): "Laser Induced Breakdown Spectroscopy (LIBS) for determination of toxic metals in liquid samples", Springer, 564\566.
- Taesam Kim and Chhiu-Tsu Lin, (2012): "Laser-Induced Breakdown Spectroscopy", chapter 5, http://dx.doi.org/10.5772/48281
- Tomoko Takahashi, et al., (2013): "Long-Pulse Laser-Induced Breakdown Spectroscopy for analysis of the composition of rock and sediment samples submerged in seawater to investigate the application of Laser-Induced Breakdown Spectroscopy", MTS, Japan, 1\2.

- Walid Tawfig, Y. Mohamed, (2007): "Calibration freell laser-induced breakdown spectroscopy (LIBS) to identify seawater", 1\2.
- Weldon, D. G., Carl, B. M. (1997): "Determination of Metallic Zinc Content of Inorganic and Organic Zinc-Rich Primers by Differential Scanning Calorimetry", Springer, UK .
- Wolfgang Demtröder, (2008): "Laser Spectroscopy, Vol. 1: Basic Principles ", 4th ed. Springer, Germany.
- www.mellesgriot.com "Basic Laser Principles", 36.2\36.3\ 36.4.
- X. Fang · S.R. Ahmad, (2011): "Detection of mercury in water by laser-induced breakdown spectroscopy with sample pre-concentration". Springer, UK, 1\2.
- Y. Godal, M.T. Taschuk, S.L. Lui, Y.Y. Tsui and R. Fedosejev, (2009): "The resonant dual-pulse technique the sensitivity of the LIBS", springer, Germany.